Atmospheric Inputs to Watersheds of the Luquillo Mountains in Eastern Puerto Rico

By Robert F. Stallard

Chapter D of
Water Quality and Landscape Processes of Four Watersheds in Eastern Puerto Rico
Edited by Sheila F. Murphy and Robert F. Stallard

Professional Paper 1789–D

U.S. Department of the Interior
U.S. Geological Survey

Contents

Figures

Tables

Abbreviations Used in This Report

μeq L^{-1}	microequivalents per liter
μm	micrometer
μmol L^{-1}	micromoles per liter
km	kilometer
km h^{-1}	kilometers per hour
m	meter
mm	millimeter
mm h^{-1}	millimeters per hour
ppmv	parts per million volume
r^2	correlation coefficient, squared
t km^{-2} yr^{-1}	metric tons per square kilometer per year
Ca*, Cl*, or Mg*	calculated nonseasalt concentration of Ca, Cl, or Mg
NADP	National Atmospheric Deposition Program
WEBB	Water, Energy, and Biogeochemical Budgets

Conversion Factors

Multiply	By	To obtain
	Length	
micrometer (μm)	0.00003937	inch (in.)
millimeter (mm)	0.03937	inch (in.)
meter (m)	3.281	foot (ft)
kilometer (km)	0.6214	mile (mi)
	Flow rate	
millimeters per hour (mm h^{-1})	0.03937	inches per hour (in h^{-1})
	Other	
metric tons per square kilometer per year (t km^{-2} yr^{-1})	2.855	short tons per square mile per year (tons mi^{-2} yr^{-1})

Atmospheric Inputs to Watersheds of the Luquillo Mountains in Eastern Puerto Rico

By Robert F. Stallard

Abstract

Twenty years of precipitation-chemistry data from the National Atmospheric Deposition Program site at El Verde, Puerto Rico, demonstrate that three major sources control the composition of solutes in rain in eastern Puerto Rico. In order of importance, these sources are marine salts, temperate contamination from the Northern Hemisphere, and Sahara Desert dust. Marine salts are a source of roughly 82 percent of the ionic charge in precipitation; marine salt inputs are greatest in January. Evaluation of 15 years of U.S. Geological Survey data for four watersheds in eastern Puerto Rico suggests that large storms, including hurricanes, are associated with exceptionally high chloride concentrations in stream waters. Some of these storms were missed in sampling by the National Atmospheric Deposition Program, and therefore its data on the marine contribution likely underestimate chloride. The marine contribution is a weak source of acidity. Temperate contamination contributes about 10 percent of the ionic charge in precipitation; contaminants are primarily nitrate, ammonia, and sulfate derived from various manmade and natural sources. Peak deposition of temperate contaminants is during January, April, and May, months in which strong weather fronts arrive from the north. Temperate contamination, a strong source of acidity, is the only component that is increasing through time. Sahara Desert dust provides 5 percent of the ionic charge in precipitation; it is strongly seasonal, peaking in June and July during times of maximum dust transport from the Sahara and sub-Saharan regions. This dust contributes, on average, enough alkalinity to neutralize the acidity in June and July rains.

Introduction

A large portion of the dissolved load in near-coastal tropical rivers comes from the atmosphere (Stallard and Edmond, 1981). This load is obtained by several processes such as precipitation, dry deposition (fallout, impaction on surfaces), and chemical fixation by biological processes or chemical-weathering reactions. Precipitation removes aerosols and some gases directly from the atmosphere, while dry deposition transfers aerosols to plant (and other) surfaces to be washed off by precipitation or condensation. Precipitation and dry deposition are commonly difficult to distinguish chemically, and only precipitation is readily sampled. Dry deposition loadings can be similar to precipitation loadings (Peters and others, 2006). Chemical fixation (the conversion of atmospheric gases into dissolved and solid compounds by chemical or biological means) is the source of much of the dissolved organic and inorganic carbon in surface waters and of considerable dissolved nitrogen. Accordingly, atmospheric inputs to rivers are commonly underestimated. In this report, atmospheric chemical inputs to eastern Puerto Rico were characterized by using relations among chemical constituents to identify constituent sources, and then using constituent deposition rates to estimate source loadings. The rainfall and runoff chemical datasets are from the National Atmospheric Deposition Program (NADP) and the U.S. Geological Survey Water, Energy, and Biogeochemical Budgets (WEBB) program. The NADP record is long (1985 to the present (2010)), but it has several large gaps. The WEBB precipitation data set (1991–1995) is more limited but helps in generalizing the data throughout the region. Runoff data are available for five rivers (Canóvanas, Cayaguás, Guabá, Icacos, and Mameyes) in four study watersheds (fig. 1).

Many of the sources of aerosols and gases that dissolve in precipitation have distinct chemical signatures. In undeveloped tropical regions within about 300 kilometers (km) of the ocean, the ocean is the largest source of solutes in rain (Stallard and Edmond, 1981). Within the ocean, solutes arise in two ways: seasalt from breaking waves and bursting bubbles, and gases emitted, generally from biological activity. The many solutes in seasalt are in characteristic proportions referred to as the "seasalt ratio." The nutrients nitrate, ammonia, silica, and phosphate are important exceptions and are typically stripped from surface seawater by biological activity. Of the major seawater ions, only sulfate has gaseous sources. Algae release to the atmosphere organic sulfur gases such as methyl sulfide, dimethyl sulfide, and carbon disulfide. Ultraviolet light quickly oxidizes these gases into precursors of sulfuric acid. Thus, the ocean can be a natural source of acid precipitation in the coastal tropics (Stallard and Edmond, 1981).

A variety of nitrogen and sulfur compounds are emitted by natural and human activities. Natural sources of sulfate include emissions from vegetation, anaerobic soils, and

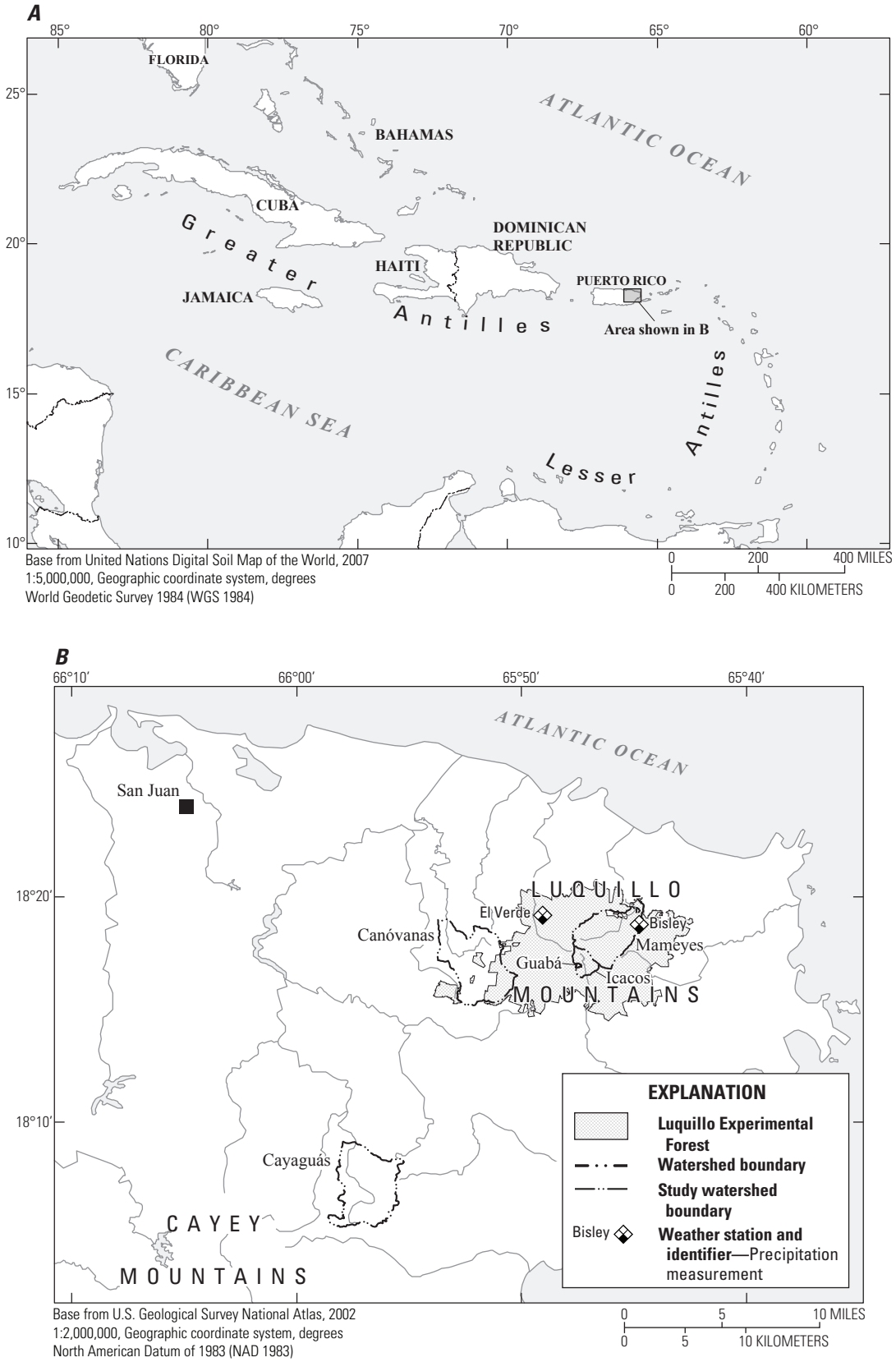

Figure 1. Location of Puerto Rico and study watersheds, eastern Puerto Rico.

volcanoes. Some ammonia and nitrate come from vegetation, biogenic emissions from soils, and from lightning (Junge, 1963). Eastern Puerto Rico is not close to any major terrestrial sources of sulfur or nitrogen, although Soufrière Hills Volcano on Montserrat (an island in the Lesser Antilles about 300 miles east-southeast of Puerto Rico), active 1995 to present, is arguably close enough to have some influence (Heartsill-Scalley and others, 2007). Human activities, especially on lands of the temperate northern hemisphere, are a major and often dominant source of nitrate, ammonia, and sulfate ions in the atmosphere, cloud waters, and precipitation (Junge, 1963; Weathers and others, 1988; Duce and others, 1991; Galloway and others, 1996; Galloway, 1998; Holland and others, 1999; Rasch and others, 2000; Rodhe and others, 2002). The sulfur and nitrogen compounds typically form aerosols that are strong acids, which are the main source of acid rain in polluted regions. Sulfur compounds, which are typically oxidized to form sulfuric acid, come from the burning of fossil fuels. Nitrogen compounds, mainly ammonium and nitrate ions, have a complex mix of sources including burning of fossil fuels and vegetation and biogenic emissions from soils enriched in nitrogen through the use of artificial fertilizers (Junge, 1963). There are no major local sources of such contamination immediately upwind (north and east) of eastern Puerto Rico (Brown and others, 1983, Ortiz-Zayas and others, 2006).

A final major source of solutes in tropical Atlantic coastal regions and islands of the Americas is dust from the Sahara Desert in Africa (Prospero and Carlson, 1972; Stallard, 2001; Reid and others, 2003a,b; Garrison and others, 2003). Fallout of dust from northern Africa blankets a zone from southern North America through Central America and northern South America (Prospero and Carlson, 1972). Seasonally averaged data from a coastal zone color-scanner satellite shows that the biggest desert-dust plume is derived from the Sahara and is carried westward by the trade winds (Stegmann and Tindale, 1999). The structure of this plume is complex and hard to characterize in detail (Reid and others, 2003a). The dust plume typically bathes Puerto Rico from June through August. Farther south, in Costa Rica and Panama, the plume is strong starting in April. The fallout of fine clay and quartz that forms the bulk of the dust is so great that it is the source of soil minerals on carbonate islands such as Bermuda (Herwitz and others, 1996). Although this dustfall has been going on for millions of years (Parkin and Shackleton, 1973), the clearing of land south of the Sahara may provide a new contribution (Lundholm, 1977; Shinn and others, 2000). Recent studies (Dunion and Velden, 2004; Evan and others, 2006) indicate a strong interaction between dry dusty air coming off the Sahara and tropical cyclones, with an inverse relation between dustiness, as measured by satellites, and cyclone activity. Sahara dust may carry pathogens that affect coral (Shinn and others, 2000), amphibians (Stallard, 2001), and people (Kuehn, 2006).

Enough dust comes from the Sahara to affect the strontium isotope composition of water and plants in the Luquillo Mountains (Pett-Ridge and others, 2009a,b) and to be a significant source of phosphate (Pett-Ridge, 2009). (The isotopic ratios of strontium from the Sahara differ from those ratios in Luquillo rocks and soils.) Pett-Ridge and others (2009b) use the Sr isotopic budget to estimate the long-term average deposition rate for Sahara dust at 21±7 metric tons per square kilometer per year (t km^{-2} yr^{-1}).

Reid and others (2003b) used x-ray fluorescence to analyze 60,500 individual particle aggregates of air-borne Sahara dust collected on a Davis rotating drum collector, which separates the dust into eight particle-size stages from 0.1 to 12 micrometers (μm). Intercorrelations among various elements provide indications of dominant particle sources. The bulk of particles sampled from air-borne Sahara dust are silicate minerals and insoluble oxides; a few percent of the total consists of sodium-chloride, calcium-rich, and calcium-sulfur particles (Reid and others, 2003b). Seasalt is the dominant source of sodium and chloride in the dust. Some salts of desert soils, such as halite (NaCl), are not readily distinguished from seasalt, especially because photochemical processes can slightly shift the original elemental proportions in air-borne seasalt (Stallard and Edmond, 1981, Reid and others, 2003b). Soluble calcium in this dust presumably comes from the calcium carbonate and calcium sulfate minerals that typically accumulate in desert soils (Birkeland, 1999, Reid and others, 2003b). Calcium carbonate reacts with and neutralizes nitric and sulfuric acids, thus generating carbon dioxide.

Elements with especially strong correlations with silicon (correlation coefficient (r^2) >0.8) were aluminum (Al/Si= 0.49, r^2=0.90), potassium (K/Si=0.059, r^2=0.92), titanium (Ti/Si=0.012, r^2=0.81), and iron (Fe/Si=0.070, r^2=0.92). Excluding sodium and chlorine, which originate largely from seasalt, the most abundant elements identified by analysis were silicon, aluminum (Al/Si=0.49), calcium (Ca/Si=0.13), sulfur (S/Si=0.1), iron (Fe/Si=0.070), magnesium (Mg/Si=0.066), and potassium (K/Si=0.059). Reid and others (2003b) estimate that more than 70 percent of dust-particle mass can be attributed to aluminosilicate clay minerals such as illite, kaolinite, and montmorillonite. Of these minerals, illite, $K_{0.6}(H_3O)_{0.4}Al_{1.3}Mg_{0.3}Fe^{2+}_{0.1}Si_{3.5}O_{10}(OH)_2 \cdot (H_2O)$, is most important. Amorphous silicon and quartz make up the next largest group, composing another 10 to 15 percent. Although these clay minerals and oxides come from desert soils, presumably they were derived from weathering during humid periods, and because these clays are solid weathering products, it is most likely that they contribute to the solid load in the rivers rather than the dissolved load (Herwitz and others, 1996).

Background—Solute Sources In Tropical Rain

The lack of local contamination sources makes the Luquillo Experimental Forest in easternmost Puerto Rico an ideal setting for studying precipitation chemistry (fig. 1). Like the prow of a ship, the Luquillo Mountains meet the east-to-west trade-wind air flow after it transits largely open ocean.

Rainfall for the region is derived from a mix of locally generated showers, tropical systems moving from the east, and frontal systems from the north (McDowell and others, 1990; Lugo and Scatena, 1992; Malmgren and others, 1998). The frontal systems are most important from December to May. Trade winds blow throughout the year but are strongest from June to November (García-Martino and others, 1996). Trade-wind meteorology has been extensively studied in the region east of Puerto Rico (Snodgrass and others, 2009, and references therein). The elevation of the trade-wind cloud base is largely controlled by sea-surface conditions, and it may be as low as 400 meters (m) but is typically around 600 m. Orographic control of rainfall is important (García-Martino and others, 1996; Murphy and Stallard, 2012); about 1,500 millimeters (mm) falls on the coast and more than 4,000 mm falls at highest elevations. More falls on the north and east sides of mountains and less on the south and west. Water from cloud interception provides 10 to 14 percent of the water budget in elfin forests (Baynton, 1968, 1969; Weaver, 1972; Brown and others, 1983; Larsen and Concepción, 1998; Schellekens and others, 1998; Eugster and others, 2006; Holwerda and others, 2006), and it may provide water to the upper portion of palo colorado forest as well.

Several studies have analyzed rain chemistry in the Luquillo Mountains (fig. 1). The best record of rainfall chemistry is from El Verde, which, with few exceptions, has been sampled by the NADP on a weekly basis since early 1985 (National Atmospheric Deposition Program (NRSP-3)/National Trends Network, 2007c, Station PR20). A 2-year gap was sustained from mid-1989 to mid-1991, starting the week that Hurricane Hugo hit, and occasional short gaps have commonly coincided with huge storms.

McDowell and others (1990) used bulk and wet precipitation from the NADP site at El Verde for 1983–1987 to identify three dominant sources of solutes in the rain: (1) marine aerosols (Na^+, K^+, Mg^{2+}, Cl^-), (2) temperate contamination (NH_4^+, SO_4^{2-}, NO_3^-), and (3) Sahara dust (K^+, Ca^{2+}, Mg^{2+}). Contaminants arrive in frontal systems from North America, and the trade winds carry contaminants from North America, Europe, and Africa. Stallard (2001) extended the analysis by using the NADP data set from 1985 through 1998 and provides a detailed analysis of trends and of the seasonality of these three sources. Stallard (2001) noted that nitrogen loading in precipitation was increasing with time, an observation also later reported by Ortiz-Zayas and others (2006). Stallard (2001) did not observe a significant contribution of K^+ and Mg^{2+} in the desert-dust component.

Heartsill-Scalley and others (2007) examined a 15-year time series, 1988–2002, of chemistry data in precipitation and throughfall sampled at the ridge above the Bisley site in the most northeast part of the Luquillo Experimental Forest (fig. 1). In addition to the constituents determined by the NADP, that study also determined total dissolved nitrogen and PO_4^{3-}. These workers found that for constituents that are common in seasalt and dust (Na^+, Ca^{2+}, Cl^-, SiO_2, and SO_4^{2-}), annual rainfall deposition is large compared with their deposition at other tropical sites, and the enrichment of throughfall by the canopy is small. Plant-active constituents (K^+, NH_4^+, NO_3^-, total dissolved nitrogen, and PO_4^{3-}) had lesser deposition in rain (rainout) than was true at many other tropical sites, and enrichment of throughfall by the canopy is large and quite variable. After hurricanes, which destroy canopy, throughfall is a greater fraction of total rainfall but it is less enriched in plant-active constituents because of less interaction with canopy. The enrichment of throughfall by plant-active solutes increased during droughts. Heartsill-Scalley and others (2007) show a weak increase in precipitation fluxes (cations, N, P) that might be associated with the Soufrière Hills Volcano.

The present paper modifies the analytical approach of Stallard (2001) to extend the analysis of the NADP data set though the time period of the WEBB research program. In addition, the effects of data gaps are examined, because the NADP data set used here, from February 12, 1985, through May 15, 2007, contains 123 data gaps ranging from 1 to 89 weeks for a total of 336 weeks out of 1,155 weeks, or 29 percent of the time. The average gap length is 2 weeks, if the four longest gaps of 11, 12, 29, and 89 weeks are excluded. Reasons for the gaps are not given except for the longest, which was caused by a lack of funding. Several gaps coincide with large storms. Large storms, especially hurricanes, defoliate the canopy, carpet the entire landscape with leaves and branches, and topple many trees (Scatena and Larsen, 1991; Schaefer and others, 2000). Collection equipment is commonly compromised, and rain samplers are typically filled with debris. Finally, access roads are sometimes blocked for days to weeks after a storm, and it is often a challenge to recover samples in a timely manner.

Methods Used to Quantify Inputs and Sources of Solutes in Precipitation

Samples at the El Verde NADP Station PR20 are collected weekly from a wet collector and analyzed using a standard protocol (National Atmospheric Deposition Program (NRSP–3)/National Trends Network, 2007a,b). The objective of this standardization is to provide a basis for comparison of major ionic constituents (H^+, Na^+, K^+, Ca^{2+}, Mg^{2+}, NH_4^+, Cl^-, SO_4^{2-}, NO_3^-) among sites and to identify trends through time. On 11 January 1994, procedures changed slightly, resulting in a slight apparent decrease in concentration of some constituents (National Atmospheric Deposition Program (NRSP–3)/National Trends Network, 2007d); however, this decrease is small compared with concentrations observed for El Verde samples. The NADP data for El Verde are available on the internet (National Atmospheric Deposition Program (NRSP–3)/National Trends Network, 2007a). The largest data gap was almost 2 years (mid-1989 to mid-1991), when samples were not collected. The NADP website provides the raw weekly data as well as monthly and annual digests of the

data. These digests were used and modified as needed for this discussion. Stallard and Edmond (1981), who collected rain samples from a ship on the Amazon River, noted that samples collected close to forest are enriched in nutrients (plant-active constituents) compared with those collected on the river hundreds of meters to kilometers from the forest edge. Accordingly, one would expect some local contamination, by bits of plant debris or insects, of these constituents in the El Verde samples, which are collected close to forest.

The chemical constituents identified by the NADP do not complete a charge balance. The concentration of hydrogen ions in rainwater is controlled by the imbalance of charge between nonreactive anions and cations and equilibration with atmospheric carbon dioxide. Accordingly, two additional constituent concentrations, bicarbonate ion (HCO_3^-) and acidity. were calculated from the hydrogen ion concentration and other constituents. Acidity is the charge difference between nonreactive anions and cations. Acidity is conservative and is the same as the negative of alkalinity (also called acid-neutralization capacity). Organic anions in tropical rainwater are quite unstable (half-lives of only a few hours (Andreae and others, 1990)), and they should not contribute to the acidity of samples that were collected during a week. For the pH range and ionic strength of the NADP samples, at equilibrium with an atmospheric partial pressure of carbon dioxide (P_{CO_2}) of 370 parts per million volume (ppmv), the concentrations of these calculated constituents are given by several equations (Stumm and Morgan, 1981; Stallard, 2001):

$$\text{Hydrogen ion: } H^+ \text{ in microequivalents per liter } (\mu\text{eq L}^{-1}) = 10^{(6-\text{pH})} \quad (1)$$

$$\text{Bicarbonate ion: } HCO_3^- = 6.36/(H^+) \quad (2)$$

$$\text{Acidity: acidity} = (\text{total anion charge of strong acids}) - (\text{total cation charge of strong bases plus } NH_4^+) \quad (3)$$

$$\text{Acidity: acidity} \approx H^+ - HCO_3^-. \quad (4)$$

These two independent calculations of acidity, equations 3 and 4, allow for a quality-control check of the overall analyses. Acidity calculated from laboratory pH is in better agreement with acidity calculated from charge balance than is acidity calculated from field pH, indicating that laboratory pH is of better data quality. When the laboratory pH is used to calculate H^+ and HCO_3^- to complete charge balances, the resultant charge balances are generally within 10 percent. Many of the samples that have excess positive charge also have excess Na^+ relative to that expected from seasalt. Likewise, many of the samples with an excess negative charge also have a sodium deficit. If the pH values are valid, this result points to analytical problems for sodium.

The NADP uses standard procedures to calculate monthly and annual digests of data (National Atmospheric Deposition Program (NRSP–3)/National Trends Network, 2007b). The monthly and annual digests prepared by NADP were used to prepare summary tables of constituent concentrations and loadings (inputs) (tables 1–4). Acidity was calculated from the analyses by using equation 3, and H^+ and HCO_3^- were, in turn, calculated from acidity using equations 2 and 4. This calculation forces a perfect charge balance and leaves problem data, such as the excess Na^+, just described, intact. The rainfall-volume-weighted averaging (calculated as the sum of weekly volume times concentration divided by total volume) of 4 to 5 weeks for each month and 52 weeks for each year reduces the influence of problem data.

Table 1. Rainfall-weighted monthly average concentration of various constituents at El Verde, Puerto Rico, derived from averaged monthly data of the National Atmospheric Deposition Program for 1983 to 2005.

[mm, millimeter; µmol L^{-1}, micromoles per liter]

Month	Rainfall (mm)	H^+ (µmol L^{-1})	Na^+ (µmol L^{-1})	K^+ (µmol L^{-1})	Mg^{2+} (µmol L^{-1})	Ca^{2+} (µmol L^{-1})	NH_4^+ (µmol L^{-1})	Cl^- (µmol L^{-1})	SO_4^{2-} (µmol L^{-1})	NO_3^- (µmol L^{-1})
January	278	9.0	134.7	3.0	15.0	3.7	2.0	153.6	13.3	5.2
February	165	9.2	108.6	2.4	11.5	3.4	2.2	122.5	11.6	5.6
March	193	9.1	82.7	2.0	9.2	3.3	1.8	97.0	9.2	4.4
April	223	13.9	57.4	1.5	6.4	2.8	3.3	67.4	10.0	6.4
May	280	10.6	51.3	1.8	5.9	2.9	2.5	61.0	8.4	5.4
June	226	2.7	64.1	1.9	7.3	6.5	2.1	74.0	8.5	5.0
July	306	2.3	66.1	1.8	7.4	6.6	1.5	75.8	8.7	3.8
August	325	4.9	46.1	1.3	5.2	4.8	1.3	54.7	7.1	3.7
September	287	6.2	70.2	1.8	8.2	4.3	1.6	83.2	8.3	3.9
October	240	7.8	38.0	0.9	4.0	2.1	1.0	44.1	5.7	3.6
November	343	7.4	62.4	1.5	6.7	1.9	0.9	72.3	6.6	2.8
December	246	10.0	90.1	2.0	9.9	2.4	1.1	105.8	9.1	3.3
Total annual	3,113									
Average annual		7.3	71.0	1.8	7.9	3.8	1.7	82.5	8.7	4.3

Table 2. Rainfall-weighted average annual concentration of various constituents at El Verde, Puerto Rico, derived from averaged annual data of the National Atmospheric Deposition Program for 1983 to 2005.

[mm, millimeter; μmol L^{-1}, micromoles per liter]

Year	Rainfall (mm)	H^+ (μmol L^{-1})	Na^+ (μmol L^{-1})	K^+ (μmol L^{-1})	Mg^{2+} (μmol L^{-1})	Ca^{2+} (μmol L^{-1})	NH_4^+ (μmol L^{-1})	Cl^- (μmol L^{-1})	SO_4^{2-} (μmol L^{-1})	NO_3^- (μmol L^{-1})
1985	3,291	4.2	61.8	1.6	7.4	4.3	0.7	74.4	7.2	1.3
1986	3,345	8.2	53.8	1.5	6.2	3.7	0.6	66.8	7.2	1.9
1987	3,892	6.7	46.5	1.2	5.6	3.7	1.1	56.0	6.9	3.2
1988	3,833	5.3	57.7	1.4	6.7	4.0	0.7	68.2	7.6	2.0
1989[1]	2,675	8.2	68.1	1.7	7.7	3.7	2.7	81.1	8.6	4.4
1991	1,178	6.9	67.5	1.8	8.1	5.3	1.1	81.2	8.5	4.8
1992	2,930	5.4	69.3	1.8	8.1	3.7	1.7	77.7	8.8	5.2
1993	2,888	7.6	61.9	2.6	7.3	3.0	2.1	73.9	7.6	4.9
1994	2,314	3.9	70.2	1.7	7.9	4.0	2.1	80.0	7.9	4.3
1995	2,624	4.2	74.6	1.7	8.0	3.8	2.9	83.4	8.4	5.2
1996	3,568	4.0	77.6	1.8	7.9	3.1	1.9	84.7	8.3	4.5
1997	2,734	11.6	55.7	1.8	6.1	3.8	1.2	68.8	8.3	4.2
1998	4,400	5.1	83.4	2.1	9.4	3.5	1.1	95.7	8.6	3.4
1999	3,153	2.0	67.2	1.6	7.0	3.8	1.7	70.7	7.7	4.8
2000	2,466	6.9	65.8	1.6	6.9	4.4	1.3	76.4	8.0	4.8
2001	2,825	9.2	67.3	1.7	6.8	4.0	1.9	79.0	8.4	5.3
2002	2,772	12.4	48.4	1.2	5.3	2.9	1.7	61.4	7.0	4.2
2003	3,266	13.6	55.4	1.4	6.1	3.5	2.3	68.6	9.0	5.0
2004	3,794	8.7	77.3	1.9	8.6	4.0	1.8	91.4	9.0	4.8
2005	3,155	9.4	99.9	2.4	11.5	4.0	2.3	113.5	12.4	6.0
2006	3,104	13.9	71.0	1.8	8.0	4.0	2.2	87.2	10.3	4.9

[1]Samples were not collected between 12 September 1989 (the day that Hurricane Hugo hit) and 4 June 1991. Rainfall totals in 1989 and 1991 are reduced accordingly.

Table 3. Rainfall-weighted monthly loadings of various constituents at El Verde, Puerto Rico, derived from averaged monthly data of the National Atmospheric Deposition Program for 1983 to 2005.

[mm, millimeter; mmol m^{-2}, millimoles per meter squared]

Month	Rainfall (mm)	H^+ (mmol m^{-2})	Na^+ (mmol m^{-2})	K^+ (mmol m^{-2})	Mg^{2+} (mmol m^{-2})	Ca^{2+} (mmol m^{-2})	NH_4^+ (mmol m^{-2})	Cl^- (mmol m^{-2})	SO_4^{2-} (mmol m^{-2})	NO_3^- (mmol m^{-2})
January	278	2.51	37.50	0.84	4.18	1.03	0.55	42.78	3.70	1.45
February	165	1.51	17.92	0.40	1.89	0.55	0.37	20.21	1.92	0.92
March	193	1.75	15.92	0.39	1.78	0.64	0.34	18.68	1.78	0.86
April	223	3.10	12.81	0.33	1.42	0.61	0.74	15.05	2.23	1.44
May	280	2.96	14.37	0.51	1.66	0.80	0.69	17.10	2.34	1.51
June	226	0.62	14.51	0.43	1.64	1.48	0.47	16.75	1.93	1.13
July	306	0.70	20.20	0.55	2.27	2.00	0.47	23.15	2.66	1.15
August	325	1.59	14.98	0.41	1.70	1.57	0.42	17.76	2.29	1.21
September	287	1.78	20.14	0.51	2.35	1.25	0.47	23.88	2.39	1.12
October	240	1.88	9.13	0.22	0.96	0.51	0.25	10.60	1.37	0.87
November	343	2.54	21.39	0.51	2.29	0.64	0.29	24.78	2.27	0.96
December	246	2.47	22.20	0.50	2.43	0.60	0.26	26.06	2.23	0.81
Total annual	3,113	23.4	221.1	5.6	24.6	11.7	5.3	256.8	27.1	13.4

Table 4. Rainfall-weighted annual loadings of various constituents at El Verde, Puerto Rico, derived from averaged annual data of the National Atmospheric Deposition Program for 1983 to 2005.

[mm, millimeter; mmol m^{-2}, millimoles per meter squared]

Year	Rainfall (mm)	H^+ (mmol m^{-2})	Na^+ (mmol m^{-2})	K^+ (mmol m^{-2})	Mg^{2+} (mmol m^{-2})	Ca^{2+} (mmol m^{-2})	NH_4^+ (mmol m^{-2})	Cl^- (mmol m^{-2})	SO_4^{2-} (mmol m^{-2})	NO_3^- (mmol m^{-2})
1985	3,291	13.7	203.4	5.4	24.2	14.0	2.4	244.9	23.6	4.4
1986	3,345	27.5	179.8	5.0	20.8	12.4	1.9	223.4	24.1	6.2
1987	3,892	26.0	180.8	4.8	21.6	14.6	4.1	217.8	27.0	12.5
1988	3,833	20.4	221.1	5.3	25.7	15.4	2.8	261.5	29.0	7.6
1989[1]	2,675	22.0	182.2	4.7	20.6	9.8	7.3	217.0	23.0	11.9
1991	1,178	8.1	79.5	2.1	9.5	6.2	1.3	95.6	10.0	5.7
1992	2,930	15.7	202.9	5.2	23.7	10.7	5.0	227.5	25.8	15.3
1993	2,888	22.0	178.8	7.4	21.1	8.6	5.9	213.4	21.8	14.2
1994	2,314	9.1	162.4	4.0	18.3	9.2	4.9	185.2	18.2	9.9
1995	2,624	11.1	195.8	4.5	20.9	10.0	7.6	218.7	22.1	13.8
1996	3,568	14.2	276.9	6.4	28.3	11.2	6.7	302.2	29.6	16.2
1997	2,734	31.8	152.3	5.0	16.6	10.4	3.2	188.2	22.7	11.4
1998	4,400	22.4	367.1	9.0	41.5	15.5	5.0	421.2	37.8	15.1
1999	3,153	6.4	211.8	5.0	21.9	12.0	5.2	222.8	24.2	15.3
2000	2,466	17.0	162.3	4.0	16.9	10.8	3.3	188.5	19.8	11.8
2001	2,825	26.0	190.1	4.8	19.3	11.2	5.5	223.1	23.7	14.9
2002	2,772	34.4	134.2	3.3	14.7	8.2	4.6	170.2	19.5	11.8
2003	3,266	44.6	181.0	4.6	19.9	11.6	7.4	224.2	29.3	16.2
2004	3,794	33.1	293.4	7.1	32.8	15.1	6.7	346.8	34.2	18.2
2005	3,155	29.8	315.2	7.5	36.2	12.7	7.2	358.1	39.1	19.0
2006	3,104	43.3	220.5	5.6	24.8	12.5	6.9	270.7	31.8	15.1

[1]Samples were not collected between 12 September 1989 (the day that Hurricane Hugo hit) and 4 June 1991. Rainfall totals in 1989 and 1991 are reduced accordingly.

Grouping Data

Procedures presented by Stallard and Edmond (1981) and Stallard (2001) were used to quantify the different sources of ions in NADP samples: marine aerosols, temperate contamination, and desert dust. Each source has at least one characteristic marker ion. In marine aerosol, Cl^-, Na^+, and Mg^{2+} ions are sufficiently abundant to be marker ions; Cl^- is most abundant and was used here. In temperate contamination, NO_3^- is the most abundant ion. NH_4^+ is also attributable to this source. In desert dust, Ca^{2+}, after correction for seasalt, is the only marker. A possible fourth source, local vegetation, is considered by using K^+ after a correction for seasalt.

Constituent groupings can be seen by using cross-correlation tables of constituent concentrations for the entire weekly data set (table 5) and for aggregated monthly mean concentrations (table 6). Rows and columns in these tables are ranked by correlation with Cl^-. For the entire data set, Cl^- correlates well with Na^+, Mg^{2+}, and SO_4^{2-} ($r^2>0.5$, indicating that more than half of the variance between Cl^- and the other constituent is shared) (Bevington and Robinson, 2003). For monthly mean data, K^+ joins this group with a strong correlation ($r^2=0.89$). The lack of such a strong correlation for weekly K^+ likely reflects major, but temporally random, local inputs. The intercorrelation among NO_3^-, NH_4^+, and SO_4^{2-} is moderate ($r^2>0.25$, more than one quarter variance shared) to strong ($r^2>0.9$, most variance is shared) in the weekly data ($0.23<r^2<0.49$) and the monthly mean data ($0.29<r^2<0.92$). Finally, Ca^{2+} does not correlate strongly with any parameter in the weekly data but anticorrelates strongly with acidity ($r^2=0.67$; $r=-0.82$) in the monthly mean data set. The groupings are illustrated as monthly mean concentrations in figure 2 and table 1 and monthly loadings in figure 2 and table 3.

Missing Samples and Big Storms

A common practice, and one used by the NADP, is to fill gaps in a long time series of data by assuming that missing data resemble data that were collected. During the WEBB Project from 1991 to 2005, in the four study watersheds and one subwatershed described here, 507 hydrologic events were sampled from 263 storms using automated samplers (appendix 1). A total of 4,894 stream-water event samples were analyzed for conductivity, most for chloride, and many for a broad suite of other constituents. Several of the largest storms during which rivers were sampled (table 7) coincide with data gaps in the NADP record. Seven storms produced stream-water chloride concentrations that were substantially greater than typical values in 117 samples. Many of these 117 samples were analyzed for a full suite of constituents, and concentrations of nearly seasalt proportions were observed for all ions that are contained abundantly in seasalt (fig. 3). Heartsill-Scalley and others (2007) note that throughfall is

Table 5. Constituent correlations for all weekly concentration data (number of samples=818), ranked by correlation with Cl^-, derived from weekly data of the National Atmospheric Deposition Program for 1983 to 2005.

[All values are squared correlation coefficients, r^2; ( ), $r^2<0$; --, not relevant]

Constituent	Cl^-	Na^+	Mg^{2+}	SO_4^{2-}	K^+	Ca^{2+}	NO_3^-	NH_4^+	Acidity
Cl^-	1	--	--	--	--	--	--	--	--
Na^+	0.97	1	--	--	--	--	--	--	--
Mg^{2+}	0.96	0.97	1	--	--	--	--	--	--
SO_4^{2-}	0.51	0.47	0.50	1	--	--	--	--	--
K^+	0.32	0.28	0.32	0.20	1	--	--	--	--
Ca^{2+}	0.17	0.16	0.19	0.22	0.11	1	--	--	--
NO_3^-	0.07	0.07	0.07	0.45	0.05	0.07	1	--	--
NH_4^+	0.02	0.02	0.02	0.23	0.02	0.01	0.49	1	--
Acidity	0.02	0.01	0.01	0.29	0.00	(0.04)	0.23	0.10	1

Table 6. Constituent correlations for aggregated monthly averaged concentration data (number of samples=12), ranked by correlation with Cl–, derived from averaged monthly data of the National Atmospheric Deposition Program for 1983 to 2005.

[All values are squared correlation coefficients, r^2; ( ), $r^2<0$; --, not relevant]

Constituent	Cl^-	Na^+	Mg^{2+}	K^+	SO_4^{2-}	NO_3^-	NH_4^+	Acidity	Ca^{2+}
Cl^-	1	--	--	--	--	--	--	--	--
Na^+	1.00	1	--	--	--	--	--	--	--
Mg^{2+}	1.00	0.99	1	--	--	--	--	--	--
K^+	0.89	0.89	0.92	1	--	--	--	--	--
SO_4^{2-}	0.78	0.79	0.80	0.83	1	--	--	--	--
NO_3^-	0.06	0.06	0.07	0.15	0.41	1	--	--	--
NH_4^+	0.01	0.01	0.02	0.07	0.29	0.93	1	--	--
Acidity	0.04	0.04	0.03	0.01	0.10	0.19	0.19	1	--
Ca^{2+}	(0.00)	(0.00)	0.00	0.02	0.00	0.01	0.01	(0.68)	1

only slightly enriched in Cl^- and other seasalt ions. Because throughfall was collected continuously from 1988 to 2002, it cannot be the source. Similarly, soils and bedrock do not retain substantial Cl^- (Stallard, 2012) and base flow is strongly enriched in alkaline ions and calcium, which are both low in concentration in the event samples (Stallard and Murphy, 2012). Groundwater cannot be a source of the high-chloride event samples. The only reasonable source of elevated Cl^- and other seasalt ions in these storms is seasalt carried inland by wind and rain. The traditional approach of assuming that missing samples resemble successfully collected samples is therefore invalid for this NADP data set, because several of the data gaps that corresponded to storms were among the nine that had exceptionally high Cl^- concentrations. One of these gaps occurred during Hurricane Georges, the largest event during this 15-year study. The second-largest storm, Hurricane Hortense, lacked both a data gap and high chloride.

By assuming that Cl^- in the stream water sampled during the storm was derived from the storm, one can integrate water and chloride discharge through the storm hydrograph to calculate total rainfall and the Cl^- concentration and loading of that rain. Two contrasting hurricanes, Hortense (September 9–10, 1996) and Georges (September 21, 1998), had comparable rainfall but show markedly contrasting Cl^- behavior (fig. 4). Georges (category 2 on the Saffir-Simpson Hurricane Wind Scale (National Oceanic and Atmospheric Administration, 2010b), winds of 154–177 kilometers per hour (km h^{-1})) was a shorter and more intense hurricane than Hortense (category 1, winds of 119–153 km h^{-1} hitting the west of Puerto Rico) (Murphy and others, 2012). Hortense, which was sampled by NADP, was a typical low-Cl^- storm, whereas Georges, which was not sampled by NADP, was a high Cl^- event. In the Mameyes watershed, the WEBB watershed closest to El Verde, Hurricane Hortense produced 333 mm total runoff with an average stream-water Cl^- concentration of 111 micromoles per liter (μmol L^{-1}) and a maximum Cl^- concentration of 253 μmol L^{-1} in the first few hours of the storm. In contrast, Hurricane Georges produced 317 mm total runoff with an average stream-water Cl^- concentration of 455 μmol L^{-1} and a maximum Cl^- concentration of 1,567 μmol L^{-1} in the first few hours of the storm. Most of the samples from Hurricane Georges were analyzed for all major constituents. The constituents in these samples are in nearly seasalt proportions, dominated by Na^+ and Cl^-, whereas the first base-flow sample collected after the storm is dominated by alkalinity and Ca^{2+} (fig. 3).

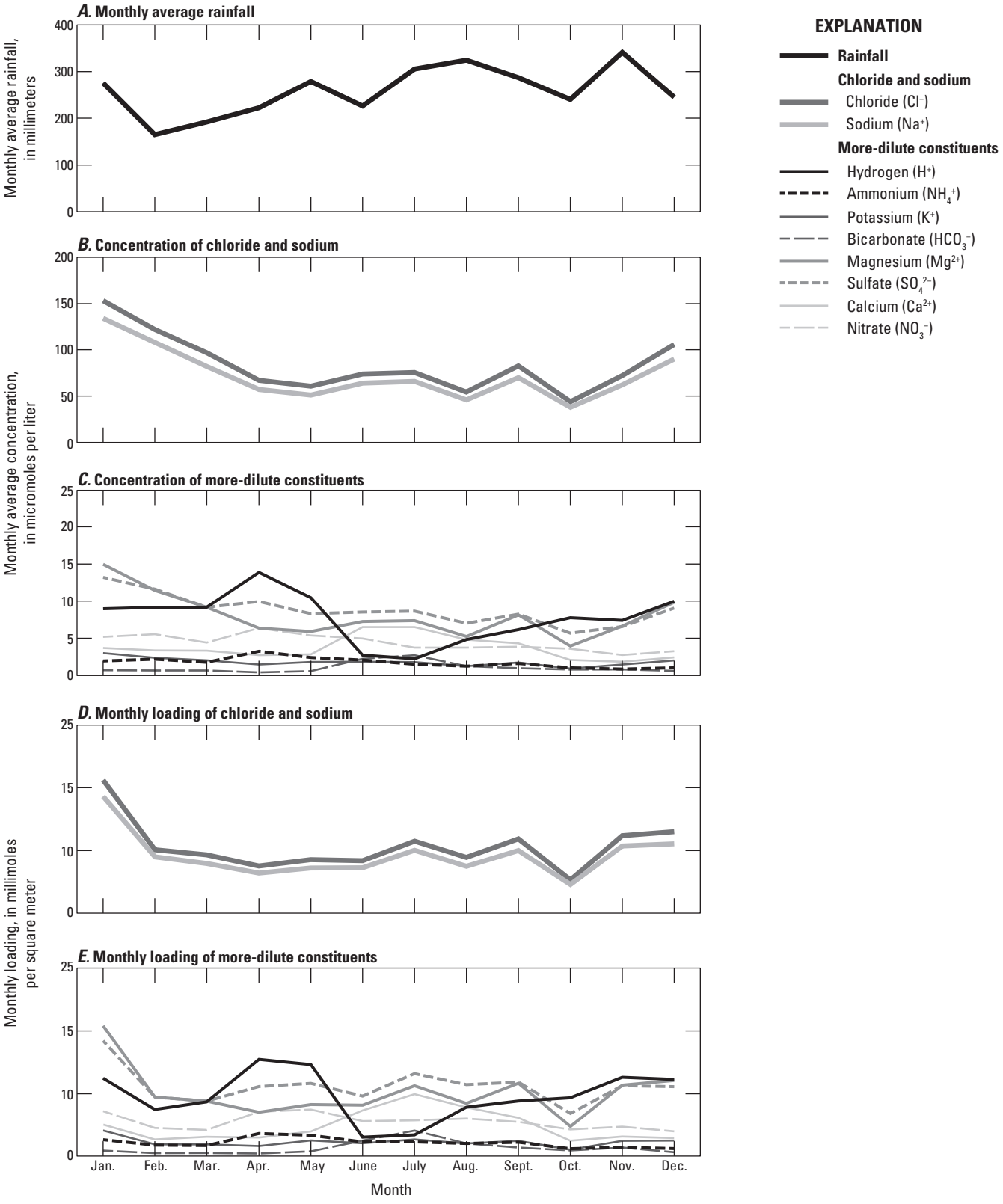

Figure 2. Aggregated monthly rainfall, monthly mean concentrations, and monthly mean loading for chemical constituents in rain sampled at the El Verde National Atmospheric Deposition Program site, eastern Puerto Rico. Light gray lines, constituents with dominantly seawater sources; dark grey lines, constituents strongly influenced by desert-dust inputs; black lines, constituents dominantly influenced by temperate-contamination sources.

Table 7. Storms that substantially affected the Water, Energy, and Biogeochemical Budgets program rivers during the period of study, 1991–2005.

[NADP, National Atmospheric Deposition Program; Can, Canóvanas; Cay, Cayaguás; Gua, Guabá; Ica, Icacos; Mam, Mameyes; n/c, normal chloride; n/g, no gap; n/s, not studied]

Date	Storm[1]	Rivers affected by the storm	Rivers with high-chloride events[2]	NADP gaps
1991–11–10	Event	Ica, Mam	n/s	Gap
1992–05–02	Event	Mam	n/c	n/g
1992–07–17	Event	Gua	n/s	n/g
1993–05–01	Event	Gua	n/c	n/g
1994–02–19	Event	Gua, Ica	n/c	n/g
1994–06–03	Minor event	Can	Can	n/g
1995–02–26	Event	Ica	n/c	n/g
1995–09–06	Hurricane Luis	Can	Can	Gap
1996–01–14	Event	Gua, Ica	n/c	n/g
1996–07–09	Hurricane Bertha	Can, Gua, Ica, Mam	Can, Gua, Ica, Mam	Gap
1996–09–10	Hurricane Hortense	Can, Cay, Gua, Ica, Mam	n/c	n/g
1997–09–25	Event	Mam	n/c	n/g
1997–10–14	Event	Gua, Ica, Cay	n/c	n/g
1998–08–25	Event	Cay	n/c	n/g
1998–09–22	Hurricane Georges	Can, Cay, Gua, Ica, Mam	Cay, Gua, Ica, Mam	Gap
1998–10–14	Event	Gua, Ica	Gua, Ica	n/g
1998–10–22	Event	Gua, Cay	Can	n/g
1998–12–02	Event	Gua, Ica	n/c	Gap
1999–11–17	Hurricane Lenny	Gua, Ica	Can	Gap
1999–12–05	Event	Gua, Ica, Mam	n/c	n/g
2000–08–22	Hurricane Debby	Gua	Can	n/g
2001–08–23	Tropical Storm Dean	Cay, Gua, Ica	n/c	n/g
2001–11–08	Cold front	Cay, Gua, Ica, Mam	n/c	n/g
2001–12–23	Event	Gua, Ica, Mam	Can	n/g
2002–05–30	Event	Gua, Ica	n/c	n/g
2003–04–18	Upper-level trough	Gua, Ica, Mam	n/c	n/g
2003–11–13	Tropical wave	Can, Cay, Gua, Ica, Mam	n/c	n/g
2004–09–16	Tropical Storm Jeanne	Can, Cay, Gua, Ica, Mam	n/s	Gap
2004–11–13	Upper-level trough	Gua, Ica, Mam	n/c	n/g
2005–10–03	Event	Cay	n/s	n/g
2005–10–11	Upper-level low	Cay, Gua, Ica	n/s	Gap
2005–10–23	Event	Cay	n/s	n/g

[1]Storms that, on the basis of runoff, could have generated landslides in at least one watershed (appendix 1, this volume), except for a minor event on the Río Canóvanas, which was the only high-chloride event sampled that did not also have substantial runoff.

[2]As identified in U.S. Geological Survey Water, Energy, and Biogeochemical Budgets program data (appendix 1, this volume).

The source of the seasalt is probably wind-generated spray. In a hurricane, mechanical energy, generated by extracting heat from the ocean, is balanced by frictional dissipation of wind energy, mostly at the sea-air interface (Emanuel, 1991). The Beaufort Scale, developed in 1805, represents a well-established description of sea-surface conditions for a wide range of wind speeds (National Oceanic and Atmospheric Administration, 2010a). For violent storms (winds of 56 to 63 knots or 104 to 117 km h^{-1}), the sea surface is described as "completely covered with long white patches of foam lying along the direction of the wind. Everywhere the edges of the wave crests are blown into froth. Visibility affected." For hurricane-force winds (at least 64 knots or 117 km h^{-1}) "the air is filled with foam and spray. Sea completely white with driving spray; visibility very seriously affected." Some of this airborne spray and foam must be incorporated into the storm. The amount of Cl^- deposited by Hurricane Georges over the entire Mameyes Basin is equivalent to 0.3 mm of seawater.

A primary reason that this phenomenon has not been described before is the unique approached used in this research that focused on event sampling (appendix 1). In this study, 332 samples that were collected at runoff rates of greater than 20 millimeters per hour (mm h^{-1}) were later analyzed for suspended sediment and a comprehensive suite of solutes. Globally, no streams have been sampled for later chemical analysis during hurricanes at runoff rates of

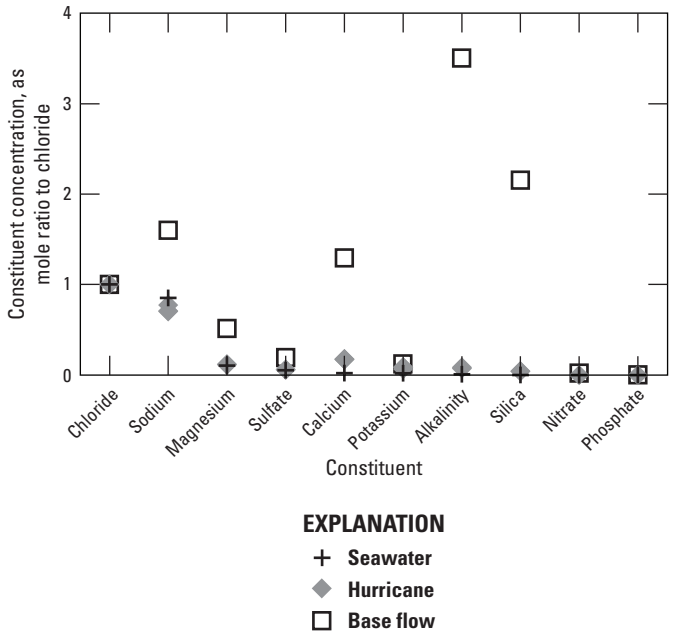

Figure 3. The three samples with the highest chloride concentrations measured for the Río Mameyes, eastern Puerto Rico, during Hurricanes Georges compared with seawater and the first base-flow sample following the hurricane, collected October 7, 1998. Chemical constituent concentrations are normalized to total chloride and are ordered by decreasing seawater concentration. The stormwater constituent proportions are close to those in seawater and are only slightly elevated in calcium, the cation most abundant in base flow.

greater than 20 mm h^{-1}; two samples were collected at about 16 mm h^{-1} by the U.S. Geological Survey in Puerto Rico in 1970 during a tropical depression (Haire, 1972). Goldsmith and others (2008) collected samples during a Typhoon Mindulle at runoff rates of as much as 7.3 mm h^{-1}, and Hicks and others collected samples during Cyclone Bola at runoff rates of as much as 4.8 mm h^{-1}.

To show the consequences of missing samples, the NADP monthly digests (fig. 5) were adjusted to include Hurricane Georges in the monthly NADP record (fig. 6). The NADP monthly data set constructs September 1998 by using only the first 2 weeks of that month. NADP also reports a total of 467 mm rain for this month; 353 mm was measured in the first 2 weeks. The National Oceanic and Atmospheric Administration rain gage at El Verde reported 730 mm for the same month (National Oceanic and Atmospheric Administration, 2008). It is not obvious why the NADP total is missing 263 mm. The difference between National Oceanic and Atmospheric Administration monthly and NADP 2-week totals is 377 mm. This 377 mm was assigned a Cl^- concentration of 455 μmol L^{-1}, the average concentration of Cl^- in the Mameyes River during Georges, along with other common seasalt constituents (Na^+, K^+, Ca^{2+}, Mg^{2+}, SO_4^{2-}) in seasalt ratios relative to Cl^-. A revised monthly average for September 1998 was then reconstructed for the NADP data set (fig. 6).

The reconstructed NADP Cl^- time series (fig. 6) demonstrates a prominent spike in September 1998. The only other comparable large spike recorded by the NADP occurred in January 2005. The January 2005 spike appears to record a series of smaller storms associated with cold fronts. Stream water was not sampled by the WEBB Project during these storms. This examination of Hurricanes Hortense and Georges demonstrates that the NADP may undersample Cl^- and other seasalt-related ions. This undersampling would be hard to reconstruct. Not only are there other high-Cl^- events that were not sampled by NADP (table 7), but two big storms were not sampled by either NADP or WEBB Project, and several storms missed by NADP had high Cl^- in some WEBB watersheds and not others (table 7). In the remaining discussion, the above correction for Hurricane Georges, which is the largest, is retained.

Estimating Source Strengths

Partitioning constituents among marine, temperate-contamination, and desert sources requires several steps. First, the marine component of all relevant constituents is calculated. NO_3^- and NH_4^+ are assumed to have zero marine contributions because of their low concentration in surface sea water. Second, nonmarine Ca^{2+} is equated with the desert-dust contribution. Finally, all NO_3^- and NH_4^+ were assumed to come from the temperate (contamination) source, because of the lack of plausible contributions from any other source.

All chloride is initially assumed to be derived from seasalt, and the chloride concentration is used to predict the marine contribution to all other ions. The seasalt contribution was then subtracted from all ions, and seasalt-corrected concentrations were obtained. Following Stallard and Edmond (1981), the concentrations that result from this calculation are designated with a superscript (*): for example, $Ca^*=Ca^{2+}-Cl^- \bullet$ (seasalt Ca:Cl). Normally, predicted measured sodium exceeded seasalt sodium, but when the reverse was true (which seldom happens and is most likely due to statistical noise or analytical error), sodium was used to calculate the seasalt contribution and a nonseasalt chloride component was calculated, to avoid negative concentrations. Elevated concentrations of nonseasalt Cl* could indicate volcanic input, as is seen in the rain of La Selva, Costa Rica (Eklund and others, 1997), or long-distance transport and photochemical processing (Stallard and Edmond, 1981). The only recent eruption near Puerto Rico was Soufrière Hills Volcano from 1996 to 1997 (Heartsill-Scalley and others, 2007), and no Cl* anomalies are noted during those times. For the NADP data set, magnesium concentrations seem slightly low and are consistently present in less-than-seasalt proportions, an unlikely situation. When a calculated Mg concentration (Mg*) is negative, again probably from analytical error, it is set to zero.

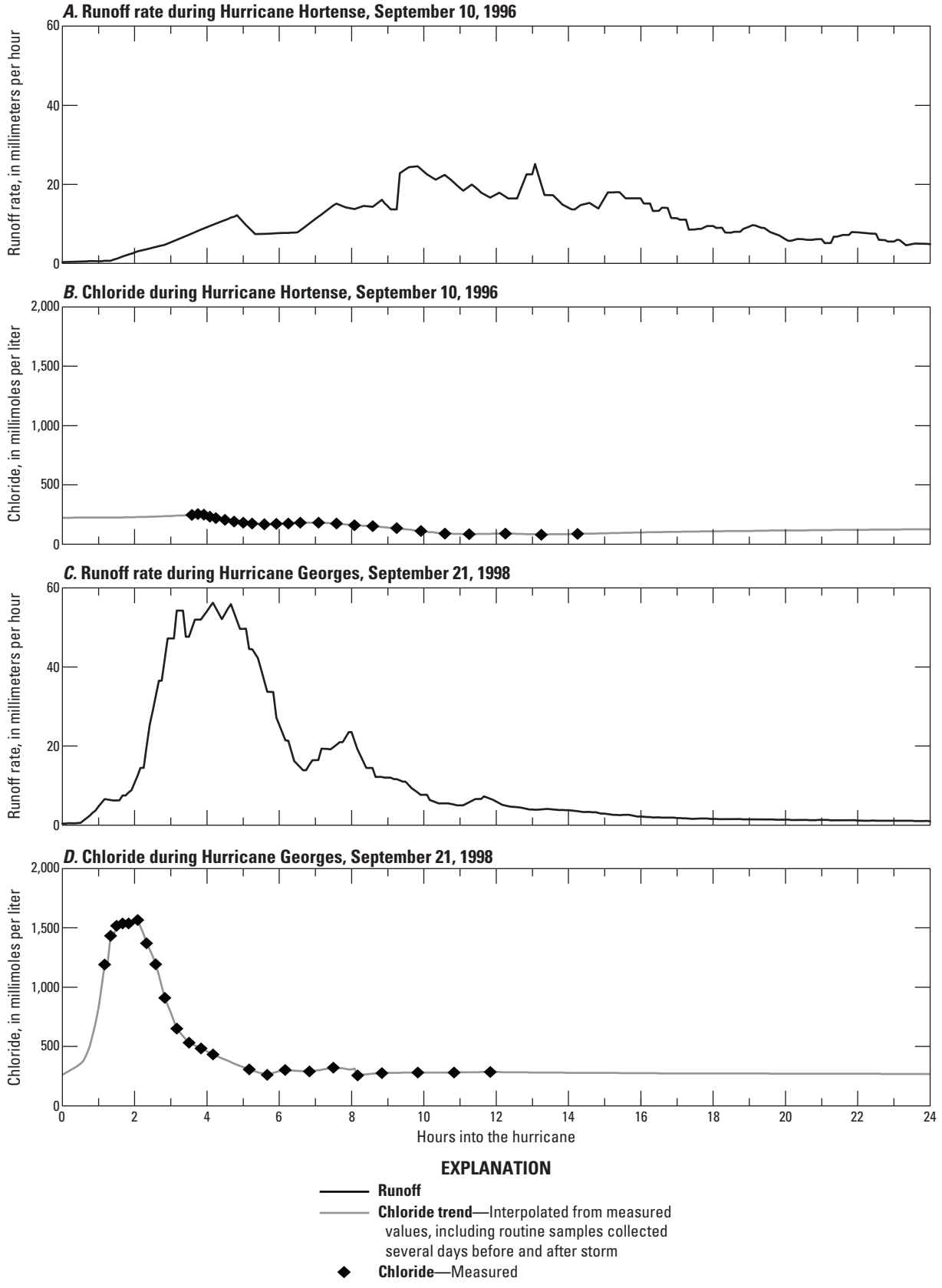

Figure 4. Time series of runoff rate and chloride concentrations measured for the Río Mameyes during Hurricanes Hortense and Georges. (Stallard and Murphy, 2012).

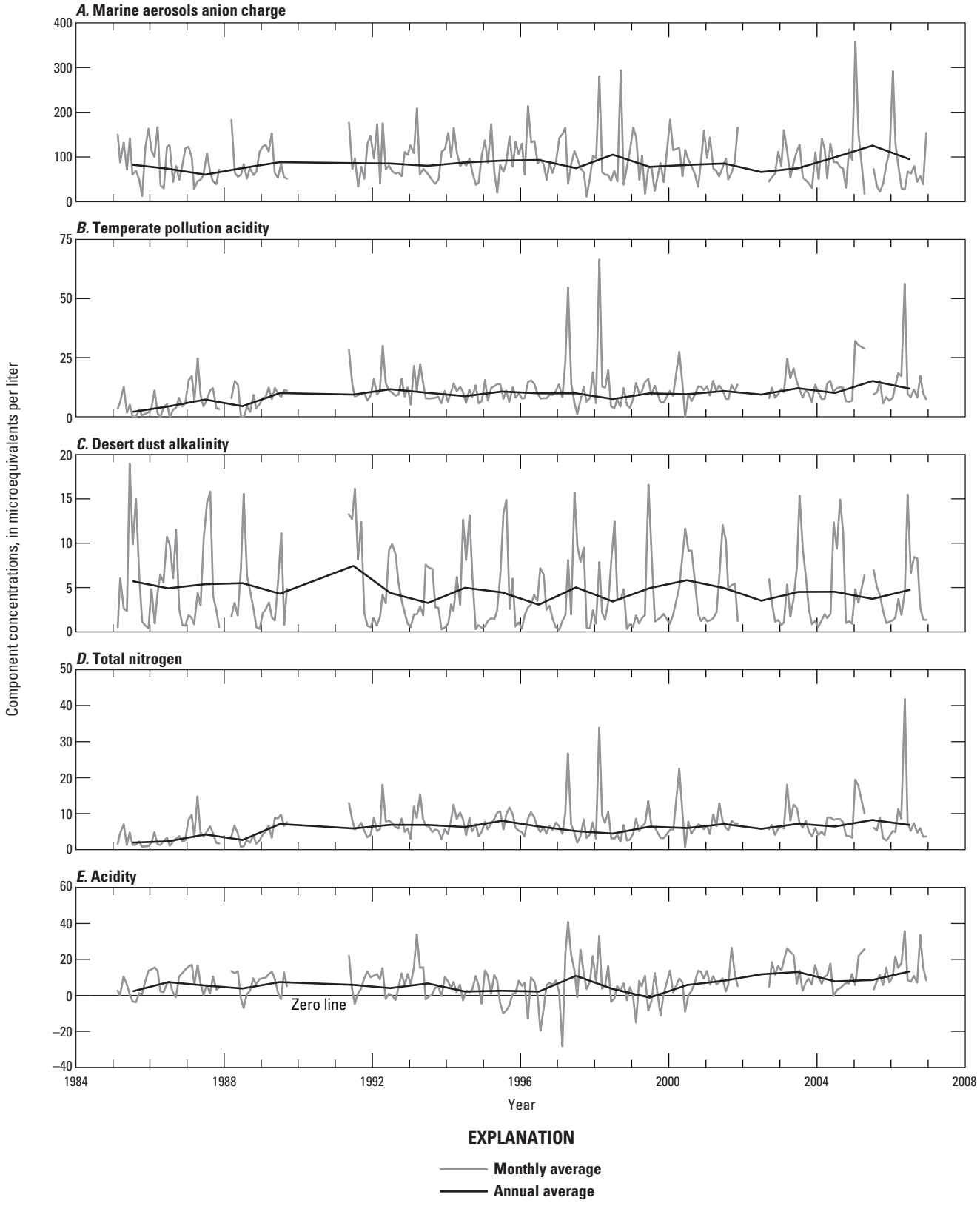

Figure 5. Time series of concentration estimates for the three primary components that contribute to rain chemistry in El Verde, Puerto Rico: *A*, marine aerosols, *B*, temperate contamination, and *C*, desert dust. *D*, total inorganic nitrogen; *E*, acidity. Negative acidity values indicate alkaline rain.

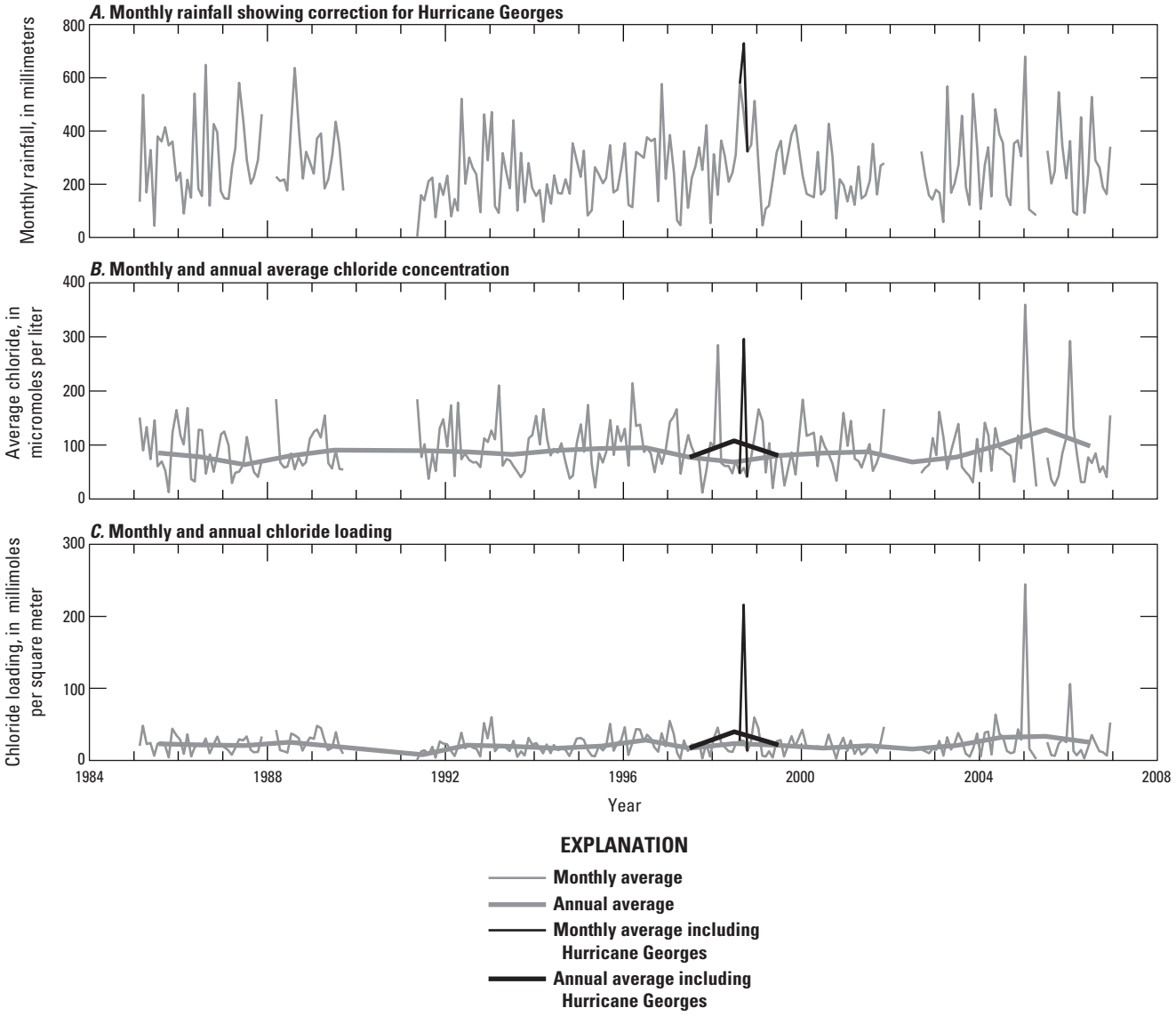

Figure 6. *A*, Monthly and annual time series of rainfall; *B*, chloride concentration; and *C*, chloride loading from the National Atmospheric Deposition Program data set for El Verde, Puerto Rico, showing effects of including data from Hurricane Georges. (Because of sample loss, rainfall amounts and rainfall chemistry were missing from the El Verde dataset for Hurricane Georges. Runoff rates and chemical samples for the Río Mameyes were used to estimate the missing data, as indicated in this graph.)

Geochemically, sulfate ion is associated with seasalt, marine-gas, temperate-contamination, and desert sources. The strong intercorrelations of SO_4^{2-} with both the seasalt (Na^+, K^+, Mg^{2+}, Cl^-) and temperate-contamination (NH_4^+, NO_3^-) groups in tables 5 and 6 support this association. Accordingly, distinguishing among the sources of SO_4^{2-} requires several steps. The marine source for SO_4^{2-} can be separated into seasalt sulfate ($SO_{4\ seasalt}^{2-}$), for which a seasalt SO_4^{2-}:Cl^- ratio can be assumed, and gas emissions ($SO_{4\ marine\ gas}^{2-}$). The SO_4^{2-} signatures of the four sources were determined for the weekly data using multiple linear regressions (Bevington and Robinson, 2003). Three properties were used as dependent variables: seasalt chloride ($Cl_{seasalt}$), nitrate (NO_3^-), and Ca*. In addition, the use of an additive constant, equivalent to assuming a "global" background SO_4^{2-} source, was tested. Most of the variance in SO_4^{2-} is accounted for by $Cl_{seasalt}$ and NO_3^-, without an additive constant. Three additional regressions were compared to evaluate whether desert or background sources of SO_4^{2-} might be important. Inclusion of the desert component, Ca*, was significant at the 76-percent level (f–test comparing a regression using $Cl_{seasalt}$ and NO_3^-, with one using $Cl_{seasalt}$, NO_3^-, and Ca*). The inclusion of a background constant was not significant. Thus, the best model is

$$SO_4^{2-}=0.060\bullet Cl_{seasalt}+0.742\bullet NO_3^-+0.229\bullet Ca^* \quad (r^2=0.778;\ n=818). \quad (5)$$

Rather than predicting SO_4^{2-} from each source using each term in equation 5, $SO_4^{2-}{}_{seasalt}$ was assumed to always be present and SO_4^* was calculated as

$$SO_4^{2-}{}_{seasalt}=0.052\bullet Cl_{seasalt} \quad (6)$$

$$SO_4^*=SO_4^{2-}-SO_4^{2-}{}_{seasalt}=0.008\bullet Cl_{seasalt}+0.742\bullet NO_3^-+0.229\bullet Ca^*. \quad (7)$$

Then SO_4^* was partitioned among the three sources according the proportions below:

$$SO_4^{2-}{}_{marine\ gas}:SO_4^{2-}{}_{temperate\ contamination}:SO_4^{2-}{}_{desert\ dust}=(0.008\bullet Cl_{seasalt}):(0.742\bullet NO_3^-):(0.229\bullet Ca^*). \quad (8)$$

The WEBB Project also collected precipitation between 1991 and 1995 (36 samples from a wet-dry collector in the Bisley area, 42 samples from a wet-dry collector near the Icacos gage, and 29 samples from a continuous collector in the central Icacos watershed). When WEBB precipitation samples are added to the regression, the best model was

$$SO_4^{2-}=0.062\bullet Cl_{seasalt}+0.677\bullet NO_3^-+0.247\bullet Ca^* \quad (r^2=0.766;\ n=925). \quad (9)$$

In this regression, somewhat more of the SO_4^{2-} is attributed to a marine gas source, and somewhat less to contamination.

For the entire El Verde NADP record, weekly concentrations of marine, temperate-pollution, and desert-dust components were calculated, as were volume-weighted monthly and annual averages of all rain samples (tables 8–13). Acidity was used to calculate H^+ and HCO_3^-, by using equations 2–4, and pH was calculated from H^+. Because alkaline desert dust reacts with acid components, thereby neutralizing some H^+,

Table 8. Averaged monthly rain chemistry from the National Atmospheric Deposition Program site at El Verde, Puerto Rico, with contributions of various sources.

[µmol L^{-1}, micromoles per liter; µeq L^{-1}, microequivalents per liter; --, not applicable]

Component	H^+ (µmol L^{-1})	Na^+ (µmol L^{-1})	K^+ (µmol L^{-1})	Mg^{2+} (µmol L^{-1})	Ca^{2+} (µmol L^{-1})	NH_4^+ (µmol L^{-1})	Acidity (µeq L^{-1})	Cl^- (µeq L^{-1})	SO_4^{2-} (µmol L^{-1})	NO_3^- (µmol L^{-1})
Average	7.3	71.0	1.8	7.9	3.8	1.7	6.4	82.5	8.7	4.3
Marine										
Seasalt	2.3	68.7	1.4	8.2	1.5	0	–0.5	80.6	4.2	0
Sulfur (sea) gases	3.4	0	0	0	0	0	1.5	0	0.8	0
Temperate	9.7	0	0	0	0	1.7	9.0	0	3.2	4.3
Desert	1.4	0	0	0	2.2	0	–3.3	0	0.6	0
Residual[1]	--	2.3	0.4	–0.3	0.0	0	–0.3	1.9	0	0

[1]All constituents not accounted for by other components; H^+ is not included because it is not a conservative constituent.

Table 9. Derived properties from monthly data of the National Atmospheric Deposition Program site at El Verde, Puerto Rico, with contributions of various sources.

[H^+ is reactive and is calculated separately for each source, the average, and the residual. $Tz^{\pm}$, total ionic charge; µeq L^{-1}, microequivalents per liter; µeq L^{-1} yr^{-1}, microequivalents per liter per year; -- not applicable]

Component	pH	$Tz^{\pm}$ (µeq L^{-1})	Percent	Slope[1] (µeq L^{-1} yr^{-1})	Slope, 95 percent error	Probability of trend[2] (percent)
Average	5.1	105.1	90	1.22	0.95	76
Marine	5.6	95.2	83	0.94	0.92	68
Seasalt	5.6	91.8	79	--	--	--
Sulfur (sea) gases	5.5	3.4	3	--	--	--
Temperate	5.0	11.4	10	0.33	0.14	97
Desert	5.9	5.8	5	–0.05	0.07	60
Residual[3]	5.6	4.5	4	–0.00	--	50

[1]Slope of the regression concentration=slope•year+intercept.

[2]Probability that the regression slope is non-zero.

[3]All ionic charge not accounted for by other components.

Table 10. Rainfall-weighted monthly average concentration of total ionic charge and acidity at El Verde, Puerto Rico, derived from averaged monthly data of the National Atmospheric Deposition Program for 1983 to 2005.

[mm, millimeter; μeq L^{-1}, microequivalents per liter; $Tz^{\pm}$, total ionic charge]

Month	Rainfall (mm)	Acidity (μeq L^{-1})				$Tz^{\pm}$ (μeq L^{-1})			
		Total	Marine	Temperate	Desert	Total	Marine	Temperate	Desert
January	278	8.3	1.3	8.3	–1.3	186.3	172.0	12.6	1.7
February	165	8.5	1.0	9.1	–1.6	154.4	136.4	13.3	2.1
March	193	8.4	0.9	9.9	–2.3	121.4	108.0	10.0	3.0
April	223	13.4	0.7	14.8	–2.1	94.5	75.0	16.5	3.0
May	280	9.9	0.6	11.8	–2.5	84.2	67.9	12.9	3.5
June	226	0.4	0.6	7.9	–8.0	99.3	79.6	9.1	10.3
July	306	–0.5	0.8	6.1	–7.5	101.1	82.7	6.9	10.3
August	325	3.6	0.6	8.8	–5.7	74.8	59.4	7.5	7.7
September	287	5.2	0.8	8.7	–4.3	105.3	91.7	8.0	5.6
October	240	7.0	0.4	8.5	–1.9	60.9	49.0	8.4	2.6
November	343	6.5	0.8	6.5	–0.8	89.5	81.5	6.8	1.0
December	246	9.4	1.1	9.0	–0.7	128.2	118.8	8.2	0.9
Annual	3,113	6.4	0.8	8.9	–3.3	106.1	91.5	9.7	4.4

Table 11. Rainfall-weighted average annual concentration of total ionic charge and acidity at El Verde, Puerto Rico, derived from averaged annual data of the National Atmospheric Deposition Program for 1983 to 2005.

[mm, millimeter; μeq L^{-1}, microequivalents per liter; $Tz^{\pm}$, total ionic charge]

Year	Rainfall (mm)	Acidity (μeq L^{-1})				$Tz^{\pm}$ (μeq L^{-1})			
		Total	Marine	Temperate	Desert	Total	Marine	Temperate	Desert
1985	3,291	2.6	1.2	5.2	–3.8	91.6	83.6	2.3	5.7
1986	3,345	7.4	1.1	9.5	–3.2	83.9	74.6	4.3	4.9
1987	3,892	5.7	0.6	9.0	–3.9	74.0	61.3	7.4	5.4
1988	3,833	4.1	1.1	6.5	–3.6	86.5	76.5	4.6	5.5
1989[1]	2,675	7.5	0.7	10.1	–3.4	103.5	89.2	10.0	4.3
1991	1,178	5.9	0.5	11.5	–6.0	103.9	87.0	9.5	7.5
1992	2,930	4.2	0.6	7.0	–3.5	101.7	85.6	11.7	4.4
1993	2,888	6.8	0.4	9.0	–2.7	94.8	81.3	10.2	3.3
1994	2,314	2.3	0.5	5.8	–4.0	101.7	88.0	8.7	5.0
1995	2,624	2.7	0.5	5.9	–3.6	107.0	91.8	10.7	4.5
1996	3,568	2.4	0.6	4.3	–2.5	107.4	94.4	9.9	3.1
1997	2,734	11.1	0.7	14.1	–3.8	90.1	75.3	9.8	5.1
1998	4,400	3.8	0.8	5.7	–2.7	117.6	106.5	7.7	3.5
1999	3,153	–1.1	0.4	2.5	–4.0	94.0	79.0	10.0	5.0
2000	2,466	6.0	0.5	10.3	–4.8	98.2	82.7	9.6	5.9
2001	2,825	8.5	0.5	12.0	–4.0	101.7	85.8	10.9	5.0
2002	2,772	11.9	0.5	14.2	–2.8	80.2	67.1	9.4	3.6
2003	3,266	13.2	0.7	15.8	–3.3	92.0	75.3	12.2	4.5
2004	3,794	8.0	0.6	11.0	–3.6	115.0	100.2	10.2	4.6
2005	3,155	8.8	1.2	10.4	–2.8	145.0	126.1	15.1	3.8
2006	3,104	13.5	1.0	16.0	–3.5	113.0	96.1	12.1	4.8

[1]Samples were not collected between 12 September 1989 (the day that Hurricane Hugo hit) and 4 June 1991. Rainfall totals in 1989 and 1991 are reduced accordingly.

Table 12. Rainfall-weighted monthly loadings of total ionic charge and acidity at El Verde, Puerto Rico, derived from averaged monthly data of the National Atmospheric Deposition Program for 1983 to 2005.

[mm, millimeter; meq m^{-2}, milliequivalents per meter squared; $Tz^{\pm}$, total ionic charge]

Month	Rainfall (mm)	Acidity (meq m^{-2})				$Tz^{\pm}$ (meq m^{-2})			
		Total	Marine	Temperate	Desert	Total	Marine	Temperate	Desert
January	278	2.31	0.36	2.30	–0.35	51.87	47.89	3.51	0.47
February	165	1.40	0.17	1.50	–0.27	25.48	22.52	2.20	0.35
March	193	1.62	0.17	1.90	–0.45	23.37	20.79	1.93	0.57
April	223	3.00	0.17	3.30	–0.46	21.09	16.74	3.68	0.66
May	280	2.79	0.18	3.31	–0.71	23.57	19.00	3.60	0.97
June	226	0.10	0.14	1.78	–1.82	22.48	18.03	2.06	2.32
July	306	–0.16	0.26	1.88	–2.29	30.88	25.27	2.10	3.14
August	325	1.17	0.18	2.85	–1.86	24.27	19.29	2.45	2.48
September	287	1.48	0.22	2.49	–1.22	30.21	26.32	2.29	1.60
October	240	1.69	0.10	2.04	–0.46	14.65	11.77	2.02	0.61
November	343	2.25	0.27	2.24	–0.26	30.68	27.94	2.32	0.35
December	246	2.31	0.28	2.21	–0.17	31.58	29.27	2.01	0.23
Annual	3,113	19.9	2.5	27.8	–10.3	330.1	284.8	30.2	13.8

Table 13. Rainfall-weighted average loadings of total ionic charge and acidity at El Verde, Puerto Rico, derived from averaged annual data of the National Atmospheric Deposition Program for 1983 to 2005.

[mm, millimeter; meq m^{-2}, milliequivalents per meter squared; $Tz^{\pm}$, total ionic charge]

Year	Rainfall (mm)	Acidity (meq m^{-2})				$Tz^{\pm}$ (meq m^{-2})			
		Total	Marine	Temperate	Desert	Total	Marine	Temperate	Desert
1985	3,291	8.7	3.9	17.2	–12.5	301.4	275.0	7.5	18.9
1986	3,345	24.9	3.7	31.9	–10.7	280.5	249.5	14.5	16.5
1987	3,892	22.3	2.4	35.2	–15.3	288.0	238.4	28.6	21.0
1988	3,833	15.8	4.4	25.1	–13.7	331.7	293.1	17.5	21.1
1989[1]	2,675	19.9	1.8	27.1	–9.0	276.9	238.6	26.7	11.6
1991	1,178	7.0	0.6	13.5	–7.1	122.4	102.5	11.1	8.8
1992	2,930	12.3	1.8	20.6	–10.1	297.9	250.7	34.2	13.0
1993	2,888	19.6	1.2	26.1	–7.7	273.7	234.7	29.5	9.4
1994	2,314	5.3	1.2	13.4	–9.3	235.3	203.6	20.2	11.5
1995	2,624	7.2	1.2	15.4	–9.5	280.7	240.8	28.2	11.7
1996	3,568	8.5	2.1	15.3	–8.8	383.3	336.8	35.4	11.1
1997	2,734	30.3	2.0	38.6	–10.3	246.4	205.7	26.9	13.8
1998	4,400	16.9	3.5	25.2	–11.8	517.5	468.5	33.7	15.3
1999	3,153	–3.4	1.4	7.9	–12.7	296.4	249.1	31.5	15.7
2000	2,466	14.7	1.2	25.3	–11.8	242.1	203.8	23.7	14.6
2001	2,825	24.0	1.4	34.0	–11.4	287.3	242.4	30.9	14.0
2002	2,772	33.0	1.3	39.5	–7.8	222.3	186.1	26.2	9.9
2003	3,266	43.1	2.4	51.5	–10.9	300.5	245.9	39.8	14.7
2004	3,794	30.3	2.4	41.7	–13.8	436.2	380.1	38.7	17.4
2005	3,155	27.6	3.7	32.8	–8.9	457.4	397.9	47.6	11.9
2006	3,104	41.9	3.1	49.6	–10.9	350.8	298.3	37.6	14.9

[1]Samples were not collected from 12 September 1989, the week that Hurricane Hugo hit, until 4 June 1991. Rainfall totals in 1989 and 1991 are reduced accordingly.

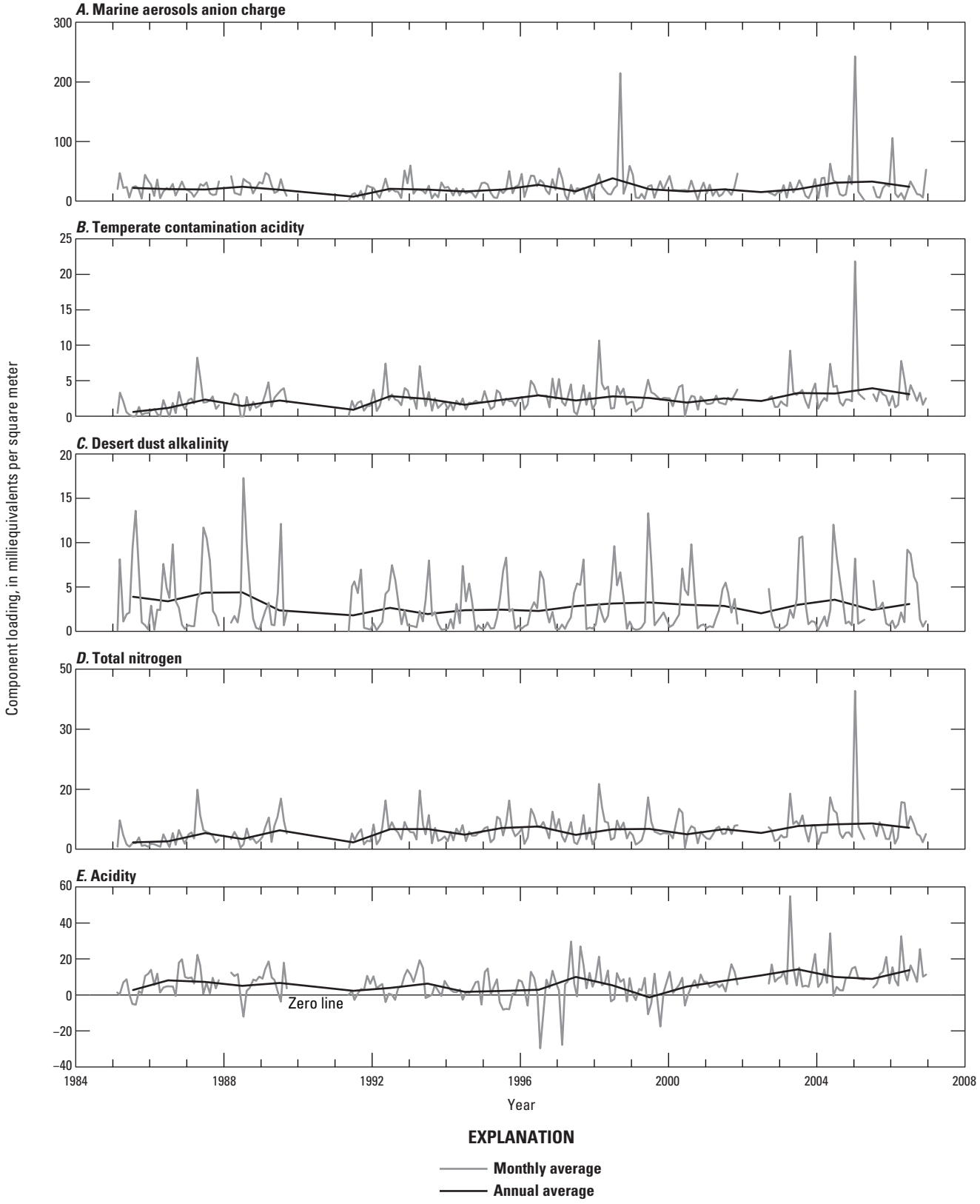

Figure 7. Time series of monthly and annual loading estimates for the three primary components that contribute to rain chemistry in El Verde, Puerto Rico: *A*, marine aerosols, *B*, temperate contamination, and *C*, desert dust. *D*, total inorganic nitrogen; *E*, acidity. Negative acidity values indicate alkaline rain.

total ion charge in rainwater is less than the charge contributed by each component (table 9). Given this caveat, the fractions of total charge attributable to these sources were as follows: marine=83 percent; temperate=10 percent; desert=5 percent; not attributed in this calculation=4 percent.

Of the nonreactive ions, K^+ has the greatest residual concentration when expressed as a fraction of total input, about 20 percent (table 9). This concentration is followed by acidity at 4 percent. This large residual indicates an additional source of K^+ beyond the three examined here. Of the constituents analyzed by both NADP and by the study of throughfall chemistry of Heartsill-Scalley and others (2007), throughfall was by far most strongly enriched in K^+, about 10 times the contribution of rainfall. Potassium was followed by Ca^{2+} and SO_4^{2-}, which are each about 1.5 times more abundant in throughfall. Accordingly, the most likely source of the residual K^+ is windblown throughfall or traces of plant matter contaminating the collector, both of which are locally derived.

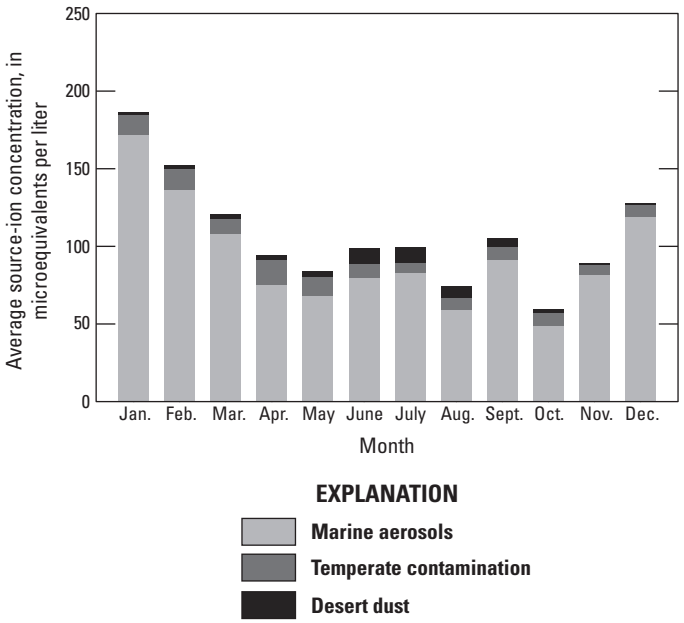

Figure 8. Aggregated monthly concentration estimates for the three primary components that contribute to rain chemistry in El Verde, Puerto Rico—marine aerosols, temperate contamination, and desert dust.

Seasonality and Trends in Inputs and Sources

The variability in the time series of weekly component concentrations (fig. 5) reflects various types of rainstorms and different air trajectories bringing air from afar into the storm. The 2-year, midrecord gap (1989–1991) was followed by more weeks with especially high concentrations of temperate contaminants, per year, than before. This abundance of especially high concentrations is reflected in the low total cation charge for 1985 to 1988 compared with later years (table 11). Although each component contains high-concentration spikes, there are too few to establish whether they are real or an artifact. When samples are averaged on a monthly basis across all years, all components show seasonality (figs. 5, 7–10). The desert-dust input, which is profoundly seasonal, appears as a major peak in concentration (figs. 5, 8) and loading (figs. 7, 9), centered on July when trade winds are strongest. The peak seasalt (marine-source) concentration (fig. 8) and loading (input) (fig. 9) is in January. Seasalt makes the smallest fractional contribution from April to July (fig. 10). The peak of hurricane season in Puerto Rico is September (table 7), but it is not reflected in a seasalt maximum. Low-chloride storms, such as Hurricane Hortense (fig. 4), presumably dominate, whereas high-chloride storms, such as Georges (fig. 4), are probably rarer and perhaps substantially undersampled. Temperate contaminants peak in January and in April and May (figs. 8, 9) under the influence of cold fronts from North America. During June to August, when the trade winds are strongest and most sustained, a large volume of contaminants may also be contributed by Europe and Africa.

The only component that shows a well-established long-term trend is temperate contamination. Stallard (2001) and Ortiz-Zayas and others (2006) note an increase in annual total-nitrogen concentrations in the NADP data set. To determine

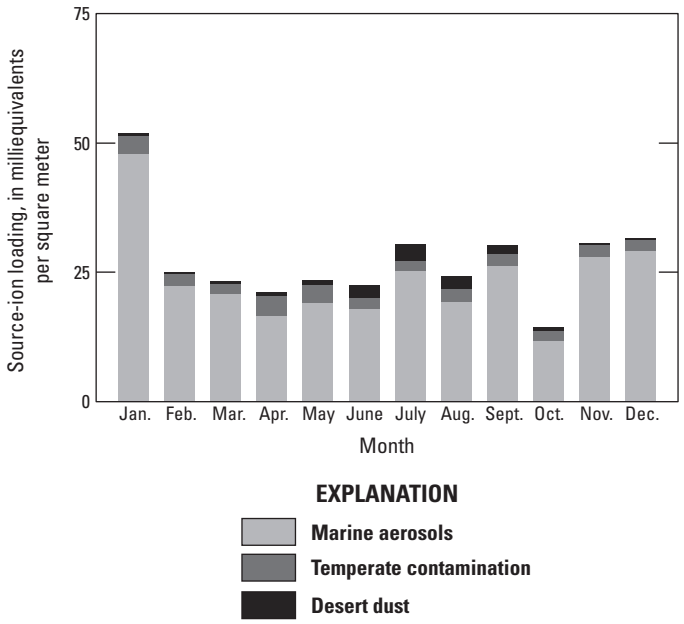

Figure 9. Aggregated monthly loading estimates for the three primary components that contribute to rain chemistry in El Verde, Puerto Rico—marine aerosols, temperate contamination, and desert dust.

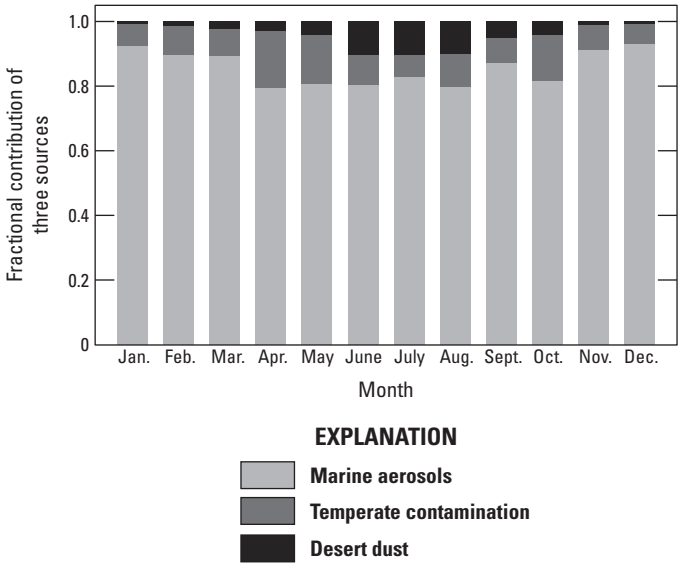

Figure 10. Fractional contribution for the three primary components that contribute to rain chemistry in El Verde, Puerto Rico—marine aerosols, temperate contamination, and desert dust.

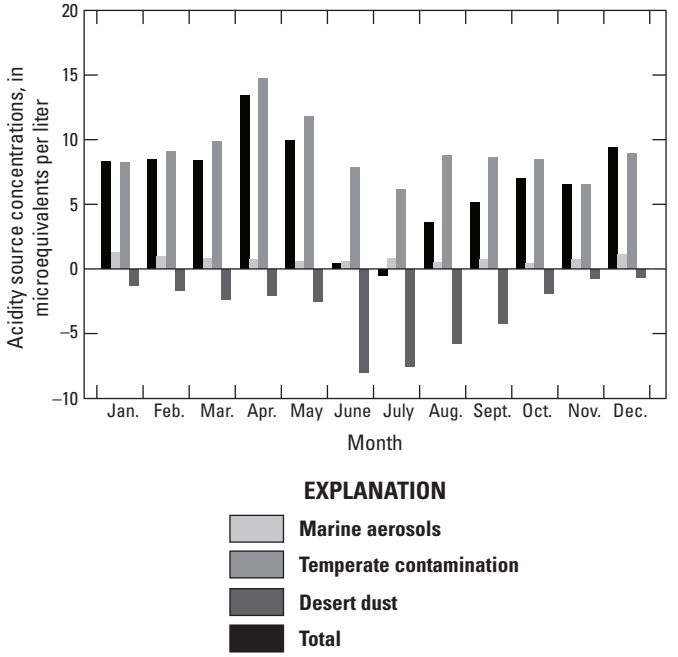

Figure 11. Monthly total acidity concentrations compared to acidity concentration estimates for the three primary components that contribute to rain chemistry in El Verde, Puerto Rico—marine, aerosols, temperate contamination, and desert dust.

significance of trends for the data in this report, the slopes of linear regressions of mean annual source concentrations compared to time were tested against a zero slope using a Student's t–test at a 95 percent confidence level (Stallard, 2001; Bevington and Robinson, 2003). Since sample collection started in 1985, there has been a significant and systematic increase in the mean-annual concentrations of ions presumably coming from the temperate contamination source (figs. 5, 7, table 9). Through time, the ratios of nitrate, ammonia, and nonmarine sulfate in rain from El Verde appear to have fairly characteristic proportions (in moles, NO_3^-:NH_4^+:SO_4^{2-}=1: 0.40: 0.74). Neither marine nor desert sources show significant trends.

Despite the increase in acid-rain components from temperate contamination, on the basis of a t–test, acidity shows no significant trend in for the period of record. Trends in acidity that are small and variable could be obscured by interactions among the three components that effectively introduce noise into the estimates of acidity (figs. 11, 12); the desert-dust input neutralizes some of the acid, and the contributions of marine-source sulfuric acid derived from algae are small and variable. Because acidity is a calculated parameter, the lack of a trend may also be confounded by the anomalous Na^+ analyses mentioned earlier. The greatest acidity, both as a concentration and a loading, develops during April and May, reflecting substantial temperate contamination. The least acidity is in June and July, reflecting reduced contamination inputs and strong loadings of desert dust.

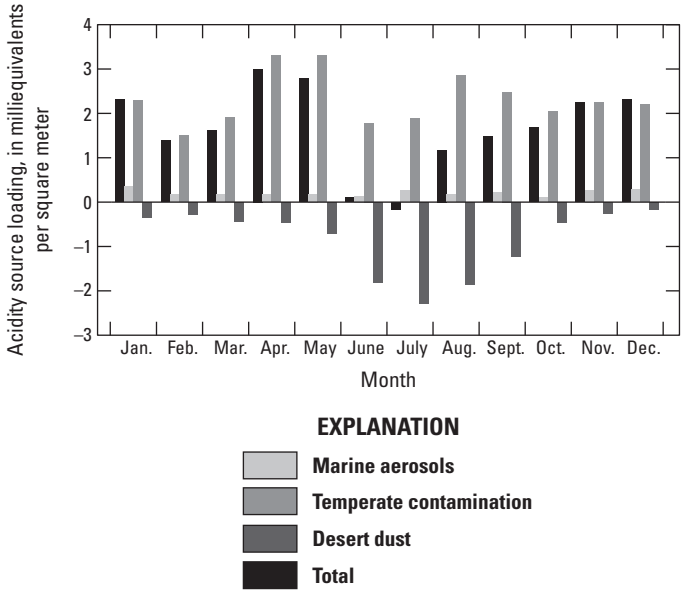

Figure 12. Monthly total acidity loadings compared to acidity loading estimates for the three primary components that contribute to rain chemistry in El Verde, Puerto Rico—marine, aerosols temperate contamination, and desert dust.

Conclusions

Three major sources control the composition of rain in eastern Puerto Rico. In order of importance, these sources are marine salts, temperate contamination, and desert dust.

Marine salts, which produce roughly 83 percent of the ionic charge, are a source of weak acidity. Peak inputs are in January, when weather in Puerto Rico is influenced by fronts and storms of Northern Hemisphere winter. Nine large storms have been associated with exceptionally high chloride concentrations in eastern Puerto Rico stream waters. Five of these storms, including the two largest, were missed in the weekly NADP sampling but not the WEBB Project sampling. Of eight hurricanes and tropical storms that affected the region, all were sampled by WEBB, but only three by NADP; three storms were sampled by neither project, and one high-chloride event, a front, was sampled by NADP but not WEBB. The NADP also did not sample Hurricane Hugo (category 3, winds of 178–209 km h^{-1}) in 1989, which was larger than Hurricane Georges. Accordingly, the marine input based exclusively on NADP data is underestimated, perhaps substantially, as is indicated by the example of Hurricane Georges explored in this report.

The temperate-contamination source includes nitrate, ammonia, and sulfate derived from anthropogenic and natural sources. Peak deposition is during January, April, and May, months in which storms and cold fronts from the north strongly influence local weather. Trade winds presumably bring contamination from Europe and Africa during the summer months. This source is the only component that is obviously increasing through time, consistent with it being a contamination source. The lesser loadings of the contamination component in the first 4 years of the record correspond with fewer samples with extreme loadings or concentrations for the same period. This trend could reflect greater incursion of contaminated air masses in subsequent years as opposed to an increase in background contamination. Temperate contamination is a strong source of acidity in rain of eastern Puerto Rico and is the chief source of acidity in the rain; by itself it would produce rain with an average pH of 5.0. Combined with other components, rain has an average pH of 5.1 (table 9), and based on application of equations 1–4, without the temperate-contamination component, rain would have an average pH of 5.6. The trend of increasingly acid rain, reflected by the increasing number of especially acid samples, may prove to be deleterious (figs. 6, 7) and by itself would justify continued long-term monitoring at this site.

The desert-dust source is strongly seasonal, peaking in June and July, during times of maximum dust transport from the Sahara and sub-Saharan regions. This dust usually contributes enough alkalinity to neutralize the acidity in June and July rains.

Acknowledgments

This chapter was greatly improved by suggestions made by Jamie B. Shanley and Martha A. Scholl of the U.S. Geological Survey.

References

Andreae, M.O., Talbot, R.W., Berresheim, H., and Beecher, K.M., 1990, Precipitation chemistry in central Amazonia: Journal of Geophysical Research v. 95, p. 16,987–17,000.

Baynton, H.W., 1968, The ecology of an elfin forest on Puerto Rico—2. The microclimate of Pico del Oeste: Journal of the Arnold Arboretum of Harvard University, v. 49, no. 4, p. 419–430.

Baynton, H.W., 1969, The ecology of an elfin forest on Puerto Rico—3. Hilltop and forest influences on the microclimate of Pico del Oeste: Journal of the Arnold Arboretum of Harvard University, v. 50, no. 1, p. 80–92.

Bevington, P.R., and Robinson, K.D., 2003, Data reduction and error analysis for the physical sciences—2: New York, McGraw Hill, 320 p.

Birkeland, P.W., 1999, Soils and geomorphology: New York, Oxford University Press, 430 p.

Brown, Sandra, Lugo, A.E., Silander, S., and Liegel, L., 1983, Research history and opportunities in the Luquillo Experimental Forest: New Orleans, La., U.S. Department of Agriculture Forest Service, Southern Forest Experimental Station General Technical Report SO–44, 128 p.

Duce, R.A., Liss, P.S., Merrill, J.T., Atlas, E.L., Buat-Menard, P., Hicks, B.B., Miller, J.M., Prospero, J.M., Arimoto, R., Church, T.M., Ellis, W., Galloway, J.N., Hansen, L., Jickells, T.D., Knap, A.H., Reinhardt, K.H., Schneider, B., Soudine, A., Tokos, J.J., Tsunogai, S., Wollast, R., and Zhou, M., 1991, The atmospheric input of trace species to the ocean: Global Biogeochemical Cycles, v. 5, no. 3, p. 193–295.

Dunion, J.P., and Velden, C.S., 2004, The impact of the Saharan air layer on Atlantic tropical cyclone activity: Bulletin of the American Meteorological Society, v. 85, no. 3, p. 353–365.

Eklund, T.J., McDowell, W.H., and Pringle, C.M., 1997, Seasonal variation of tropical precipitation chemistry—La Selva, Costa Rica: Atmospheric Environment, v. 31, no. 23, p. 3903–3910.

Emanuel, K.A., 1991, The theory of hurricanes: Annual Reviews of Fluid Mechanics, v. 23, p. 179–196.

Eugster, Werner, Burkard, R., Holwerda, F., Scatena, F.N., and Bruijnzeel, L.A., 2006, Characteristics of fog and fogwater fluxes in a Puerto Rican elfin cloud forest: Agricultural and Forest Meteorology, v. 139, p. 288–306.

Evan, A.T., Dunion, J., Foley, J.A., Heidinger, A.K., and Velden, C.S., 2006, New evidence for a relationship between Atlantic tropical cyclone activity and African dust outbreaks: Geophysical Research Letters, v. 33, L19813, p. 1–5.

Galloway, J.N., 1998, The global nitrogen cycle—Changes and consequences: Environmental Pollution, v. 102, p. 15–24.

Galloway, J.N., Howarth, R.W., Michaels, A.F., Nixon, S.W., Prospero, J.M., and Dentener, F.J., 1996, Nitrogen and phosphorus budgets of the North Atlantic Ocean and its watershed: Biogeochemistry, v. 35, p. 3–25.

García-Martino, A.R., Warner, G.S., Scatena, F.N., and Civco, D.L., 1996, Rainall, runoff, and elevation relationships in the Luquillo Mountains of Puerto Rico: Caribbean Journal of Science, v. 32, no. 4, p. 413–424.

Garrison, V.H., Shinn, E.A., Foreman, W.T., Griffin, D.W., Holmes, C.W., Kellogg, C.A., Majewski, M.S., Richardson, L.L., Ritchie, K.B., and Smith, G.W., 2003, African and Asian dust—From desert soils to coral reefs: Bioscience, v. 53, no. 5, p. 469–480.

Goldsmith, S.T., Carey, A.E., Lyons, W.B., Kao, S.-J., Lee, T.-Y., and Chen, J., 2008, Extreme storm events, landscape denudation, and carbon sequestration—Typhoon Mindulle, Choshui River, Taiwan: Geology, v. 36, no. 6, p. 483–486.

Haire, W.J., 1972, Flood of October 5–10, 1970: Puerto Rico, Commonwealth of Puerto Rico Water-Resources Bulletin 12, 42 p.

Heartsill-Scalley, Tamara, Scatena, F.N., Estrada, C., McDowell, W.H., and Lugo, A.E., 2007, Disturbance and long-term patterns of rainfall and throughfall nutrient fluxes in a subtropical wet forest in Puerto Rico: Journal of Hydrology, v. 333, p. 472–485.

Herwitz, S.R., Muhs, D.R., Prospero, J.M., Mahan, S., and Vaughn, B., 1996, Origin of Bermuda's clay-rich Quaternary paleosols and their paleoclimatic significance: Journal of Geophysical Research, v. 101, no. D18, p. 23,389–23,400.

Holland, E.A., Dentener, F.J., Braswell, B.H., and Sulzman, J.M., 1999, Contemporary and preindustrial global reactive nitrogen budgets: Biogeochemistry, v. 46, p. 7–43.

Holwerda, Friso, Burkard, R., Eugster, W., Scatena, F.N., Meesters, A.G.C.A., and Bruijnzeel, L.A., 2006, Estimating fog deposition at a Puerto Rican elfin cloud forest site—Comparison of the water budget and eddy covariance methods: Hydrological Processes, v. 20, p. 2669–2692.

Junge, C.E., 1963, Air chemistry and radioactivity: New York, Academic Press, 382 p.

Kuehn, B.M., 2006, Desertification called global health threat: Journal of the American Medical Association, v. 295, no. 21, p. 2463–2465.

Larsen, M.C., and Concepción, I.M., 1998, Water budgets of forested and agriculturally developed watersheds in Puerto Rico, *in* Segarra-García, R.I., ed., Tropical hydrology and Caribbean water resources, International Symposium on Tropical Hydrology, 3d, and Caribbean Islands Water Resources Congress, 5th, San Juan, Puerto Rico, July 13–16, 1998, Proceedings: American Water Resources Association, p. 199–204.

Lugo, A.E., and Scatena, F.N., 1992, Epiphytes and climate change research in the Caribbean—A proposal: Selbyana, v. 13, p. 123–130.

Lundholm, Bengt, 1977, Ecology and dust transport, *in* Morales, Christer, ed., Saharan dust—Mobilization, transport, deposition; papers and recommendations from a workshop held in Gothenburg, Sweden, 25–28 April 1977: Gothenburg, SCOPE 14, p. 61–68.

Malmgren, B.A., Winter, A., and Chen, D., 1998, El Niño—Southern oscillation and North Atlantic oscillation control of climate in Puerto Rico: Journal of Climate, v. 11, p. 2713–2717.

McDowell, W.M., Gines-Sánchez, C., Asbury, C.E., and Pérez, C.R.R., 1990, Influence of sea-salt aerosols and long-range transport on precipitation chemistry at El Verde, Puerto Rico: Atmospheric Environment, v. 24A, p. 2813–2821.

Murphy, S.F., and Stallard, R.F., 2012, Hydrology and climate of four watersheds in eastern Puerto Rico, ch. C *in* Murphy, S.F., and Stallard, R.F., eds., Water quality and landscape processes of four watersheds in eastern Puerto Rico: U.S. Geological Survey Professional Paper 1789, p. 43–84.

Murphy, S.F., Stallard, R.F., Larsen, M.C., and Gould, W.A., 2012, Physiography, geology, and land cover of four watersheds in eastern Puerto Rico, ch. A *in* Murphy, S.F., and Stallard, R.F., eds., Water quality and landscape processes of four watersheds in eastern Puerto Rico: U.S. Geological Survey Professional Paper 1789, p. 1–24.

National Oceanic and Atmospheric Administration, 2008, National Climate Data Center, accessed May 16, 2008, at *http://www.ncdc.noaa.gov/oa/ncdc.html*

National Oceanic and Atmospheric Administration, 2010a, Beaufort Wind Scale, accessed September 30, 2010, at *http://www.srh.noaa.gov/mfl/?n=beaufort*

National Oceanic and Atmospheric Administration, 2010b, The Saffir-Simpson Hurricane Wind Scale, accessed September 30, 2010, at *http://www.nhc.noaa.gov/pdf/sshws.pdf*

National Atmospheric Deposition Program (NRSP–3)/ National Trends Network, 2007a, National Atmospheric Deposition Program (NADP/NTN), accessed September 13, 2007, at *http://nadp.sws.uiuc.edu/*

National Atmospheric Deposition Program (NRSP–3)/ National Trends Network, 2007b, NADP/NTN overview and history, accessed September 13, 2007, at *http://nadp.sws.uiuc.edu/NADP/*

National Atmospheric Deposition Program (NRSP–3)/ National Trends Network, 2007c, NADP/NTN site list, accessed September 13, 2007, at *http://nadp.sws.uiuc.edu/sites/latlong.asp*

National Atmospheric Deposition Program (NRSP–3)/ National Trends Network, 2007d, Notification of important change in NADP/NTN procedures on 11 January 1994, accessed September 13, 2007, at *http://nadp.sws.uiuc.edu/documentation/advisory.html*

Ortiz-Zayas, J.R., Cuevas, E., Mayol-Bracero, O.L., Donoso, L., Trebs, I., Figueroa-Nieves, D., and McDowell, W.H., 2006, Urban influences on the nitrogen cycle in Puerto Rico: Biogeochemistry, v. 79, p. 109–133.

Parkin, D.W., and Shackleton, N.J., 1973, Trade wind and temperature correlations down a deep-sea core off the Saharan coast: Nature, v. 245, p. 91–92.

Peters, N.E., Shanley, J.B., Aulenbach, B.T., Webb, R.M., Campbell, D.H., Hunt, R., Larsen, M.C., Stallard, R.F., Troester, J.W., and Walker, J.F., 2006, Water and solute mass balance of five small, relatively undisturbed watersheds in the U.S.: Science of the Total Environment, v. 358, p. 221–242.

Pett-Ridge, J.C., 2009, Contributions of dust to phosphorus cycling in tropical forests of the Luquillo Mountains, Puerto Rico: Biogeochemistry, v. 96, no. 1, p. 63–80.

Pett-Ridge, J.C., Derry, L.A., and Barrows, J.K., 2009a, Ca/Sr and $^{87}Sr/^{86}Sr$ ratios as tracers of Ca and Sr cycling in the Río Icacos watershed, Luquillo Mountains, Puerto Rico: Chemical Geology, v. 94, no. 1, p. 64–80.

Pett-Ridge, J.C., Derry, L.A., and Kurtz, A.C., 2009b, Sr isotopes as a tracer of weathering processes and dust inputs in a tropical granitoid watershed, Luquillo Mountains, Puerto Rico: Geochimica et Cosmochimica Acta, v. 73, p. 25–43.

Prospero, J.M., and Carlson, T.N., 1972, Vertical and areal distribution of Saharan dust over the western equatorial North Atlantic Ocean: Journal of Geophysical Research, v. 77, p. 5255–5265.

Rasch, P.J., Barth, M.C., Kiehl, J.T., Schwartz, S.E., and Benkovitz, C.M., 2000, A description of the global sulfur cycle and its controlling processes in the National Center for Atmospheric Research Community Climate Model, Version 3: Journal of Geophysical Research, v. 105, p. 1367–1385.

Reid, J.S., Kinney, J.E., Westphal, D.L., Holben, B.N., Welton, E.J., Tsay, S., Eleuterio, D.P., Campbell, J.R., Christopher, S.A., Colarco, P.R., Jonsson, H.H., Livingston, J.M., Maring, H.B., Meier, M.L., Pilewskie, P., Prospero, J.M., Reid, E.A., Remer, L.A., Russell, P.B., Savoie, D.L., Smirnov, A., and Tanré, D., 2003a, Analysis of measurements of Saharan dust by airborne and ground-based remote sensing methods during the Puerto Rico Dust Experiment (PRIDE): Journal of Geophysical Research, v. 108, no. D19, 8586, p. 1–27.

Reid, E.A., Reid, J.S., Meier, M.M., Dunlap, M.R., Cliff, S.S., Broumas, A., Perry, K., and Maring, H., 2003b, Characterization of African dust transported to Puerto Rico by individual particle and size segregated bulk analysis: Journal of Geophysical Research, v. 108, no. D19, 8591, p. 1–22.

Rodhe, Henning, Dentener, F., and Schulz, M., 2002, The global distribution of acidifying wet deposition: Environmental Science and Technology, v. 36, p. 4382–4388.

Scatena, F.N., and Larsen, M.C., 1991, Physical aspects of hurricane Hugo in Puerto Rico: Biotropica, v. 23, p. 317–323.

Schaefer, D.A., McDowell, W.H., Scatena, F.N., and Asbury, C.E., 2000, Effects of hurricane disturbance on stream water concentrations and fluxes in eight tropical forest watersheds of the Luquillo Experimental Forest, Puerto Rico: Journal of Tropical Ecology, v. 16, p. 189–207.

Schellekens, Jaap, Bruijnzeel, L.A., Wickel, A.J., Scatena, F.N., and Silver, W.L., 1998, Interception of horizontal precipitation by elfin cloud forest in the Luquillo Mountains, eastern Puerto Rico, *in* Schemenauer, R.S., and Bridgman, H.A., eds., International Conference on Fog and Fog Collection, 1st, Vancouver, Canada, July 19–24, 1998, Proceedings: Ottawa, Canada, International Development Research Centre, p. 29–32.

Shinn E.A., Smith G.W., Prospero, J.M., Betzer, P., Hayes, M.L., Garrison, V.H., and Barber, R.T., 2000, African dust and the demise of Caribbean coral reefs: Geological Research Letters, v. 27, no. 19, p. 3029–3032.

Snodgrass, E.R., di Girolamo, L., and Rauber, R.M., 2009, Precipitation characteristics of trade wind clouds during RICO derived from radar, satellite, and aircraft measurements: Journal of Applied Meteorology and Climatology, v. 84, p. 464–483.

Stallard, R.F., 2001, Possible environmental factors underlying amphibian decline in eastern Puerto Rico—Analysis of U.S. government data archives: Conservation Biology, v. 15, no. 4, p. 943–953.

Stallard, R.F., 2012, Weathering, landscape equilibrium, and carbon in the four watersheds in eastern Puerto Rico, ch. H *in* Murphy, S.F., and Stallard, R.F., eds., Water quality and landscape processes of four watersheds in eastern Puerto Rico: U.S. Geological Survey Professional Paper 1789, p. 199–248.

Stallard, R.F., and Edmond, J.M., 1981, Geochemistry of the Amazon—1. Precipitation chemistry and the marine contribution to the dissolved load at the time of peak discharge: Journal of Geophysical Research—Oceans and Atmospheres, v. 86, no. NC10, p. 9844–9858.

Stallard, R.F., and Murphy, S.F., 2012, Water quality and mass transport in four watersheds in eastern Puerto Rico, ch. E *in* Murphy, S.F., and Stallard, R.F., eds., Water quality and landscape processes of four watersheds in eastern Puerto Rico: U.S. Geological Survey Professional Paper 1789, p. 113–152.

Stegmann, P.M., and Tindale, N.W., 1999, Global distribution of aerosols over the open ocean as derived from the coastal zone color scanner: Global Biogeochemical Cycles, v. 13, no. 2, p. 383–397.

Stumm, Werner, and Morgan, J.J., 1981, Aquatic chemistry: New York, John Wiley, 780 p.

Weathers, K.C., Likens, G.E., Bormann, F.H., Bicknell, S.H., Bormann, B.T., Daube, B.C., Jr., Eaton, J.S., Galloway, J.N., Keene, W.C., Kimball, K.D., McDowell, W.H., Siccama, T.G., Smiley, D., and Tarrant, R.A., 1988, Cloud water chemistry from ten sites in North America: Environmental Science and Technology, v. 22, p. 1018–1026.

Weaver, P.L., 1972, Cloud moisture interception in the Luquillo Mountains of Puerto Rico: Caribbean Journal of Science, v. 12, no. 3–4, p. 129–144.